

Order and quantum phase transitions in the cuprate superconductors

Subir Sachdev*

Department of Physics, Yale University, P.O. Box 208120, New Haven CT 06520-8120

(Dated: October 28, 2002)

It is now widely accepted that the cuprate superconductors are characterized by the same long-range order as that present in the Bardeen-Cooper-Schrieffer (BCS) theory: that associated with the condensation of Cooper pairs. We argue that many physical properties of the cuprates require interplay with additional order parameters associated with a proximate Mott insulator. We review a classification of Mott insulators in two dimensions, and contend that the experimental evidence so far shows that the class appropriate to the cuprates has collinear spin correlations, bond order, and confinement of neutral, spin $S = 1/2$ excitations. Proximity to second-order quantum phase transitions associated with these orders, and with the pairing order of BCS, has led to systematic predictions for many physical properties. We use this context to review the results of recent neutron scattering, fluxoid detection, nuclear magnetic resonance, and scanning tunnelling microscopy experiments.

Contents

I. INTRODUCTION	1
II. BCS THEORY	2
III. MOTT INSULATORS	3
A. Magnetically ordered states	4
1. Collinear spins, $\mathbf{N}_1 \times \mathbf{N}_2 = 0$	5
2. Non-collinear spins, $\mathbf{N}_1 \times \mathbf{N}_2 \neq 0$	5
B. Paramagnetic states	5
1. Bond-ordered states: confined spinons	6
2. Topological order: free spinons	8
C. Connections between magnetically ordered and paramagnetic states	9
1. Collinear spins and bond order	10
2. Non-collinear spins and topological order	10
IV. ORDER IN STATES PROXIMATE TO MOTT INSULATORS	11
A. Tuning order by means of a magnetic field	12
B. Detecting topological order	14
C. Non magnetic impurities	15
D. STM studies of the vortex lattice	15
V. A PHASE DIAGRAM WITH COLLINEAR SPINS, BOND ORDER, AND SUPERCONDUCTIVITY	16
VI. OUTLOOK	18
Acknowledgments	19
References	19

I. INTRODUCTION

The discovery of high temperature superconductivity in the cuprate series of compounds by Bednorz and Müller (1986) has strongly influenced the development of condensed matter physics. It stimulated a great deal

of experimental work on the synthesis and characterization of a variety of related intermetallic compounds. It also reinvigorated theoretical study of electronic systems with strong correlations. Technological applications of these materials have also appeared, and could become more widespread.

Prior to this discovery, it was widely assumed that all known superconductors, or superfluids of neutral fermions such as ^3He , were described by the theory of Bardeen, Cooper and Schrieffer (BCS) (Bardeen *et al.*, 1957). Certainly, the quantitative successes of BCS theory in describing an impressive range of phenomena in the lower temperature superconductors make it one of the most successful physical theories ever proposed. Soon after the discovery of the high temperature superconductors, it became clear that many of their properties, and especially those at temperatures (T) above the superconducting critical temperature (T_c), could not be quantitatively described by the BCS theory. Overcoming this failure has been an important motivation for theoretical work in the past decade.

One of the purposes of this article is to present an updated assessment of the applicability of the BCS theory to the cuprate superconductors. We will restrict our attention to physics at very low temperature associated with the nature of the ground state and its elementary excitations. This will allow us to focus on sharp, qualitative distinctions. In particular, we will avoid the regime of temperatures above T_c , where it is at least possible that any failure of the BCS theory is a symptom of our inability to make accurate quantitative predictions in a strong coupling regime, rather than our having missed a qualitatively new type of order. Also, while this article will present a unified view of the important physics of the cuprate superconductors, it is not a comprehensive review, and it does not attempt to reflect the state of the field by representing the variety of viewpoints that have been taken elsewhere in the literature.

The primary assertions of this article are as follows. At the lowest energy scales, the longest length scales, in

*Electronic address: subir.sachdev@yale.edu

the absence of strong external perturbations, and at ‘optimal’ carrier concentrations and above, all experimental indications are that the cuprate superconductors can indeed be described in the framework of the BCS theory: the theory correctly captures the primary order parameter of the superconducting state, and the quantum numbers of its elementary excitations. However, many experiments at lower doping concentrations and at shorter length scales require one or more additional order parameters, either conventional (*i.e.* associated with the breaking of a symmetry of the Hamiltonian) or ‘topological’ (see Section III.B.2 below). These order parameters are best understood and classified in terms of the physics of ‘Mott insulators,’ a topic which will be discussed in greater detail below. The importance of the Mott insulator was stressed by Anderson (1987). Our understanding of Mott insulators, and of their classification into categories with distinct physical properties has advanced greatly in the last decade, and a sharper question of experimental relevance is: which class of Mott insulators has its ‘order’ present in the cuprate superconductors? As we shall discuss below, the evidence so far supports a class quite distinct from that implied in Anderson’s proposal (Sachdev and Read, 1991).

How can the postulated additional order parameters be detected experimentally? In the simplest case, there could be long-range correlations in the new order in the ground state: this is apparently the case in $\text{La}_{2-\delta}\text{Sr}_\delta\text{CuO}_4$ at low carrier concentrations, and we will describe recent experiments which have studied the interplay between the new order and superconductivity. However, the more common situation is that there are no long range correlations in any additional order parameter, but the ‘fluctuating’ order is nevertheless important in interpreting certain experiments. A powerful theoretical approach for obtaining semi-quantitative predictions in this regime of fluctuating order is provided by the theory of quantum phase transitions: imagine that we are free to tune parameters so that ultimately the new order does acquire long range correlations somewhere in a theoretical phase diagram. A quantum critical point will separate the phases with and without long-range order: identify this critical point and expand away from it towards the phase with fluctuating order, which is the regime of experimental interest (Chubukov *et al.*, 1994a; Sachdev and Ye, 1992); see Fig 1. An illuminating discussion of fluctuating order near quantum critical points (along with a thorough analysis of many recent experiments which has some overlap with our discussion here) has been provided recently by Kivelson *et al.* (2002a).

An especially important class of experiments involve perturbations which destroy the superconducting order of the BCS state *locally* (on the scale a few atomic spacings). Under such situations the theory outlined above predicts that the order of the Mott insulator is revealed in a halo surrounding the perturbation, and can, in principle, be directly detected in experiments. Perturbations of this type are Zn impurities substituting on the Cu sites, and

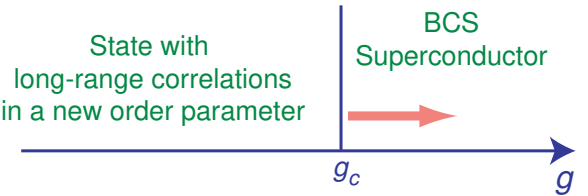


FIG. 1 Our theoretical strategy for describing the influence of a new order parameter in a BCS superconductor. Here g is some convenient coupling constant in the Hamiltonian, and we imagine that the superconductor of physical interest is a BCS superconductor with $g > g_c$. Theoretically, it is useful to imagine that we can tune g to a value smaller than g_c where there are long-range correlations in a new order parameter. Having identified and understood the quantum phase transition at $g = g_c$, we can expand away from it back towards the BCS superconductor (as indicated by the thick arrow) to understand the influence of quantum fluctuations of the new order parameter. This approach is most effective when the transition at $g = g_c$ is second order, and this will usually be assumed in our discussion. Note that the horizontal axis need not be the concentration of mobile carriers, and it may well be that the superconductor of physical interest does not exhibit the $g < g_c$ state at any carrier concentration.

the vortices induced by an applied magnetic field. We shall discuss their physics below.

To set the stage for confrontation between theory and experiment, we review some essential features of the BCS theory in Section II, and introduce key concepts and order parameters in the theory of Mott insulators in Section III. We will combine these considerations in our discussion of doped Mott insulators in Section IV, which will also include a survey of some experiments. A theoretical phase diagram which encapsulates much of the physics discussed here appears in Section IV, while Section VI concludes with a discussion on possible directions for future work.

II. BCS THEORY

In BCS theory, superconductivity arises as an instability of a metallic Fermi liquid. The latter state is an adiabatic continuation of the free electron model of a metal, in which all single particle states, labeled by the Bloch crystal momentum \vec{k} , inside the \vec{k} -space Fermi surface are occupied by electrons, while those outside remain empty. With $c_{\vec{k}\sigma}^\dagger$ the creation operator for an electron with momentum \vec{k} and spin projection $\sigma = \uparrow\downarrow$, a reasonable description of the Fermi liquid is provided by the free electron Hamiltonian

$$H_0 = \sum_{\vec{k}\sigma} (\varepsilon_{\vec{k}} - \mu) c_{\vec{k}\sigma}^\dagger c_{\vec{k}\sigma}, \quad (1)$$

where $\varepsilon_{\vec{k}}$ is the energy-momentum dispersion of the single-particle Bloch states and μ is the chemical potential; the locus of points with $\varepsilon_{\vec{k}} = \mu$ defines the Fermi

surface. Changes in electron occupation numbers near the Fermi surface allow low energy processes which are responsible for the conduction properties of metals.

BCS realized that an arbitrarily weak attractive interaction between the electrons would induce the electrons near the Fermi surface to lower their energy by binding into pairs (known as Cooper pairs) (Cooper, 1956). BCS also proposed a mechanism for this attractive interaction: the exchange of a low energy phonon between two electrons, along with the rapid screening of the repulsive Coulomb interaction by the other electrons, leads to a residual attractive interaction near the Fermi surface. We regard this mechanism of electron pairing as a specific sidelight of BCS theory for good metals, and not an essential characterization of the BCS state. Indeed in liquid ^3He , the pairing is believed to arise from exchange of spin fluctuations ('paramagnons'), but the resulting superfluid state has many key similarities to the superconducting metals.

In the BCS ground state, the Cooper pairs undergo a process of condensation which is very closely related to the Bose-Einstein condensation of non-interacting bosons. Two well separated Cooper pairs obey bosonic statistics when adiabatically exchanged with each other, but their behavior is not simply that of point-like Bose particles when their internal wavefunctions overlap—the constituent electrons become important at these short scales; however it is the long distance bosonic character which is crucial to the appearance of a condensate of Cooper pairs. In the original Bose-Einstein theory, the zero momentum boson creation operator can be replaced by its *c*-number expectation value (due to the occupation of this state by a macroscopic number of bosons); similarly, the BCS state is characterized by the expectation value of the creation operator of a Cooper pair with zero center of mass momentum:

$$\left\langle c_{\vec{k}\uparrow}^\dagger c_{-\vec{k}\downarrow}^\dagger - c_{\vec{k}\downarrow}^\dagger c_{-\vec{k}\uparrow}^\dagger \right\rangle \propto \Delta_{\vec{k}} \equiv \Delta_0 (\cos k_x - \cos k_y). \quad (2)$$

The functional form of (2) in spin and \vec{k} -space carries information on the internal wavefunction of the two electrons forming a Cooper pair: we have displayed a spin-singlet pair with a *d*-wave orbital wavefunction on the square lattice, as is believed to be the case in the cuprates (Scalapino, 1995; Tsuei and Kirtley, 2000).

Along with (2) as the key characterization of the ground state, BCS theory also predicts the elementary excitations. These can be separated into two types: those associated with the motion of center of mass, \vec{R} , of the Cooper pairs, and those in which a pair is broken. The center of mass motion (or superflow) of the Cooper pairs is associated with a slow variation in the phase of the pairing condensate $\Delta_0 \rightarrow \Delta_0 e^{i\phi(\vec{R})}$: the superconducting ground state has $\phi(\vec{R}) = \text{constant}$ independent of \vec{R} (and thus long-range order in this phase variable), while a slow variation leads to an excitation with superflow. A vortex excitation is one in which this phase has a non-trivial winding, while the superflow has a non-zero circu-

lation:

$$\int_C d\vec{R} \cdot \nabla \phi = 2\pi n_v \quad (3)$$

where n_v is the integer-valued vorticity, and C is a contour enclosing the vortex core. A standard gauge invariance argument shows that each such vortex must carry a total magnetic flux of $n_v hc/(2e)$, where the $2e$ in the denominator represents the quantum of charge carried by the "bosons" in the condensate. Excitations which break Cooper pairs consist of multiple $S = 1/2$ fermionic quasiparticles with dispersion

$$E_{\vec{k}} = \sqrt{(\epsilon_{\vec{k}} - \mu)^2 + |\Delta_{\vec{k}}|^2}, \quad (4)$$

and these reduce to the particle and hole excitations around the Fermi surface when $\Delta_0 \rightarrow 0$.

All indications from experiments so far are that the cuprate superconductors do have a ground state characterized by (2), and the elementary excitations listed above. However, BCS theory does make numerous other predictions which have been successfully and thoroughly tested in the low temperature superconductors. In particular, an important prediction is that if an external perturbation succeeds in destroying superconductivity by sending $|\Delta_0| \rightarrow 0$, then the parent Fermi surface, which was swallowed up by the Cooper instability, would reappear. This prediction is quite different from the perspective discussed earlier, in which we argued for the appearance of a halo of order linked to the Mott insulator.

III. MOTT INSULATORS

The Bloch theory of metals also specified conditions under which crystalline materials can be insulating: if, after filling the lowest energy bands with electrons, all bands are either fully occupied or completely empty, then there is no Fermi surface, and the system is an insulator. However, some materials are insulators even though these conditions are not satisfied, and one-electron theory would predict partially filled bands: these are Mott insulators. Correlations in the motion of the electrons induced by their Coulomb interactions are crucial in preventing metallic conduction.

One of the parent compounds of the cuprate superconductors, La_2CuO_4 , is a simple example of a Mott insulator. The lowest energy electronic excitations in this material reside on the Cu $3d_{x^2-y^2}$ orbitals, which are located on the vertices of a square lattice. The crystal has a layered structure of stacked square lattices, with only a weak amplitude for electron hopping between successive layers. (We shall neglect the interlayer coupling and focus on the physics of a single square lattice in the remainder of this article.) After accounting for the ionization states of the other ions in La_2CuO_4 , there turns out to be exactly one electron per unit cell available to occupy the Cu $3d_{x^2-y^2}$ band. With two available spin states, this

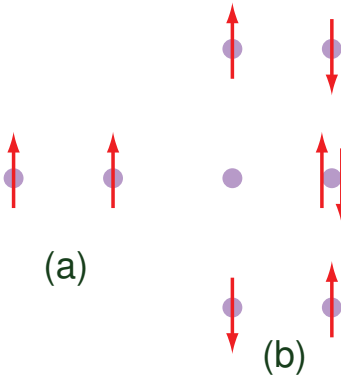


FIG. 2 Motion of the two ferromagnetically aligned spins in (a) is prohibited by the Pauli principle. In contrast, the antiferromagnetically aligned spins at the top and bottom in (b) can access a high energy intermediate state (shown in the middle of (b)) and so undergo an exchange process.

band can accommodate two electrons per unit cell, and so is half-filled, and should have a metallic Fermi surface. Nevertheless, La_2CuO_4 is a very good insulator. The reason for this insulating behavior can be understood quite easily from a simple classical picture of electron motion in the presence of the Coulomb interactions. Classically, the ground state consists of one electron localized on each of the $3d_{x^2-y^2}$ orbitals: this state minimizes the repulsive Coulomb interaction energy. Any other state would have at least one orbital with two electrons, and one with no electrons: there is a large energetic penalty for placing two electrons so close to each other, and this prohibits motion of electrons across the lattice: hence the Mott insulator.

Let us now look at the quantum theory of the Mott insulator more carefully. While charge fluctuations on each site are expensive, it appears that the spin of the electron can be rotated freely and independently on each site. However, in the quantum theory virtual charge fluctuations do occur, and these lead to residual “super-exchange” interactions between the spins (Anderson, 1959). We represent the spin on the Cu site j by the $S = 1/2$ spin operator \mathbf{S}_j ; the effective Hamiltonian that describes the spin dynamics then takes the form

$$H = \sum_{i < j} J_{ij} \mathbf{S}_i \cdot \mathbf{S}_j + \dots \quad (5)$$

where the J_{ij} are short-ranged exchange couplings and the ellipses represent possible multiple spin couplings, all of which preserve full $SU(2)$ spin rotation invariance. Because the Pauli principle completely prohibits charge fluctuations between two sites if they have parallel spin electrons, while they are only suppressed by the Coulomb repulsion if they have opposite spins (see Fig 2), we expect an antiferromagnetic sign $J_{ij} > 0$, so that nearby spins prefer opposite orientations. Classifying quantum ground states of models like (5) is a problem of considerable complexity, and has been the focus of extensive

research in the last decade. We summarize the current understanding below.

In keeping with the spirit of this article, we characterize ground states of H by a number of distinct order parameters. We only discuss states below which have long-range correlation in a single order parameter; in most cases, co-existence of multiple order parameters is also allowed (Balents *et al.*, 1999; Senthil and Fisher, 2000), but we will ignore this complexity here. Our list of order parameters is not exhaustive, and we restrict our attention to the most plausible candidates (in the author’s opinion) for short-range J_{ij} .¹

Although our discussion below will refer mainly to Mott insulators, we will also mention ground states of non-insulating systems with mobile charge carriers: the order parameters we use to characterize Mott insulators can be applied more generally to other systems, and this will be done in more detail in Section IV.

A. Magnetically ordered states

Such states are obtained by examining H for the case of large spin S on each site: in this limit, the \mathbf{S}_j can be taken as classical c -numbers, and these take a definite non-zero value in the ground state. More precisely, the $SU(2)$ spin rotation symmetry of H is spontaneously broken in the ground state by the non-zero values of $\langle \mathbf{S}_j \rangle$, which are chosen to minimize the energy of H . We consider only states without a net ferromagnetic moment ($\sum_j \langle \mathbf{S}_j \rangle = 0$), and this is expected because $J_{ij} > 0$. The pattern of non-zero $\langle \mathbf{S}_j \rangle$ can survive down to $S = 1/2$, and this is often found to be the case, although quantum fluctuations do significantly reduce the magnitude of $\langle \mathbf{S}_j \rangle$.

An especially important class of magnetically ordered states² is characterized by a single ordering wavevector

¹ An order that has been much discussed in the literature, which we do not discuss here, is that associated with the staggered flux state (Affleck and Marston, 1988), and the related algebraic spin liquid (Rantner and Wen, 2001; Wen, 2002a). The low energy theory of these states includes a gapless U(1) gauge field, and it has been argued (Sachdev and Park, 2002) that instantons, which are allowed because the underlying lattice scale theory has a compact gauge symmetry, always proliferate and render these unstable towards confining states (of the type discussed in Section III.B.1) in two spatial dimensions. However, states with a gapless U(1) gauge field are allowed in three spatial dimensions (Motrunich and Senthil, 2002; Wen, 2002b).

² Magnetically ordered states with the values of $\langle \mathbf{S}_j \rangle$ non-coplanar (*i.e.* three dimensional spin textures) are not included in this simple classification. Their physical properties are expected to be similar to those of the non-collinear case discussed in Section III.A.2 in that quantum fluctuations of such a state lead to a paramagnet with topological order. However, this paramagnet is likely to have also a broken time-reversal symmetry.

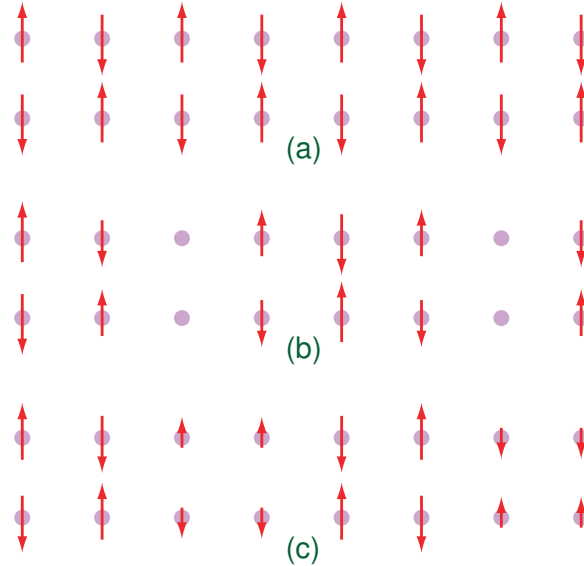


FIG. 3 States with collinear magnetic order on a square lattice with unit lattice spacing and wavevectors (a) $\vec{K} = (\pi, \pi)$, (b) and (c) $\vec{K} = (3\pi/4, \pi)$. Shown are the values of (6) on the square lattice sites \mathbf{r}_j . A single unit cell is shown for the latter two states; they are crystallographically inequivalent and have different reflection planes: in (b) the reflection planes are on certain sites, while in (c) they are at the midpoint between two sites.

\vec{K} :

$$\langle \mathbf{S}_j \rangle = \mathbf{N}_1 \cos(\vec{K} \cdot \vec{r}_j) + \mathbf{N}_2 \sin(\vec{K} \cdot \vec{r}_j) \quad (6)$$

where \vec{r}_j is the spatial location of the site j , and $\mathbf{N}_{1,2}$ are two fixed vectors in spin space. We list two key sub-categories of magnetically ordered Mott insulators which obey (6):

1. Collinear spins, $\mathbf{N}_1 \times \mathbf{N}_2 = 0$

In this situation, the mean values of the spins in (6) on all sites j are either parallel or anti-parallel to each other. The undoped insulator La_2CuO_4 is of this type³ with $\vec{K} = (\pi, \pi)$; see Fig 3a. Insulating states with static holes appeared in Zaanen and Gunnarsson (1989), Machida (1989), Schulz (1989), and Poilblanc and Rice (1989) with ordering wavevectors which move continuously away from (π, π) . Another important illustrative example is the case $\vec{K} = (3\pi/4, \pi)$. Such a wavevector could be preferred in a Mott insulator by longer range J_{ij} in (5), but in practice it is found in a non-insulating state obtained by doping La_2CuO_4 with a suitable density of

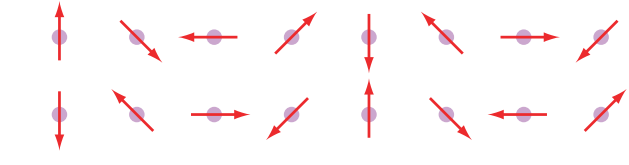


FIG. 4 A state with non-collinear magnetic order on the square lattice defined by (6) and (7) with wavevector $\vec{K} = (3\pi/4, \pi)$.

mobile carriers (Kivelson and Emery, 1996; Martin *et al.*, 2000; Seibold *et al.*, 1998; Tranquada *et al.*, 1995; Wakimoto *et al.*, 2001, 1999; White and Scalapino, 1998a,b, 1999)—we can crudely view the mobile carriers as having induced an effective longer range exchange between the spins. Two examples of states with this value of \vec{K} are shown in Fig 3, a *site*-centered state with $\mathbf{N}_2 = 0$ in Fig 3b, and a *bond*-centered state with $\mathbf{N}_2 = (\sqrt{2} - 1)\mathbf{N}_1$ in Fig 3c. (The states have planes of reflection symmetry located on sites and the centers of bonds respectively, and so are crystallographically inequivalent. Also, these inequivalent classes are only present if the wavevector \mathbf{K} is commensurate with the underlying lattice.)

2. Non-collinear spins, $\mathbf{N}_1 \times \mathbf{N}_2 \neq 0$

Now the spin expectation values in (6) lie in a plane in spin space, rather than along a single direction. For simplicity, we will only consider the simplest, and most common, case of non-collinearly ordered state, in which

$$\mathbf{N}_1 \cdot \mathbf{N}_2 = 0 \quad ; \quad \mathbf{N}_1^2 = \mathbf{N}_2^2 \neq 0, \quad (7)$$

and then the values of $\langle \mathbf{S}_j \rangle$ map out a circular spiral (Shraiman and Siggia, 1988, 1989), as illustrated in Fig 4.

B. Paramagnetic states

The other major class of states comprises those having

$$\langle \mathbf{S}_j \rangle = 0, \quad (8)$$

and the ground state is a total spin singlet.⁴ Loosely speaking each spin \mathbf{S}_j finds a partner, say $\mathbf{S}_{j'}$, and the two pair up to form a singlet valence bond

$$\frac{1}{\sqrt{2}} (|\uparrow\rangle_j |\downarrow\rangle_{j'} - |\downarrow\rangle_j |\uparrow\rangle_{j'}). \quad (9)$$

³ For this special value of \vec{K} on the square lattice, and with the origin of \mathbf{r} co-ordinates on a lattice site, (6) is actually independent of \mathbf{N}_2

⁴ In a finite system with an even number of spins, the magnetically ordered ground state also has total spin zero. However, to obtain a state which breaks spin rotation symmetry as in (6), it is necessary to mix in a large number of nearly degenerate states which carry non-zero total spin. The paramagnetic does not have such higher spin states available at low energy in a finite system.

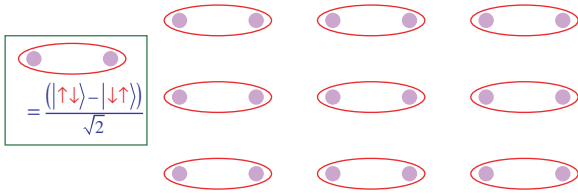


FIG. 5 A crude variational wavefunction of a bond-ordered paramagnetic state. The true ground state will have fluctuations of the singlet bonds about the configuration shown here, but its pattern of lattice symmetry breaking will be retained. In other words, each bond represented by an ellipse above will have the same value of $\langle Q_a(\vec{r}_j) \rangle$, and this value will be distinct from that associated with all other bonds. This pattern of symmetry breaking is represented more abstractly in Fig 6a.

Of course, there are many other choices for the partner of spin \mathbf{S}_j , and in the Feynman path integral picture we imagine that the pairing configuration fluctuates in quantum imaginary time; this is the ‘resonating valence bond’ picture of Pauling (1949), Fazekas and Anderson (1974), and Anderson (1987). However, there is a great of structure and information contained in the manner in which this fluctuation takes place, and research (Chubukov *et al.*, 1994b,c; Read and Sachdev, 1991; Sachdev and Read, 1991) delineating this structure has led to the following classification of paramagnetic Mott insulators.

1. Bond-ordered states: confined spinons

This class of states can be easily understood by the caricature of its wavefunction shown in Fig 5: here each spin has chosen its valence bond partner in a regular manner, so that there is a long-range ‘crystalline’ order in the arrangement of valence bonds. This ordering of bonds clearly breaks the square lattice space group symmetries under which the Hamiltonian is invariant. Of course, the actual wavefunction for any realistic Hamiltonian will have fluctuations in its valence bond configuration, but the pattern of lattice symmetry breaking implied by Fig 5 will be retained in the true bond-ordered ground state. We can make this precise by examining observables which are insensitive to the electron spin direction: the simplest such observables we can construct from the low energy degrees of freedom of the Mott insulator are *bond* variables, which are a measure of the exchange energy between two spins:

$$Q_a(\vec{r}_j) \equiv \mathbf{S}_j \cdot \mathbf{S}_{j+a}. \quad (10)$$

Here a denotes displacement by the spatial vector \vec{r}_a , and so the spins above are at the spatial locations \vec{r}_j and $\vec{r}_j + \vec{r}_a$. We will mainly consider bond order with $\vec{r}_a \neq 0$, but note that the on-site variable $Q_0(\vec{r}_j)$, with $\vec{r}_a = 0$, is

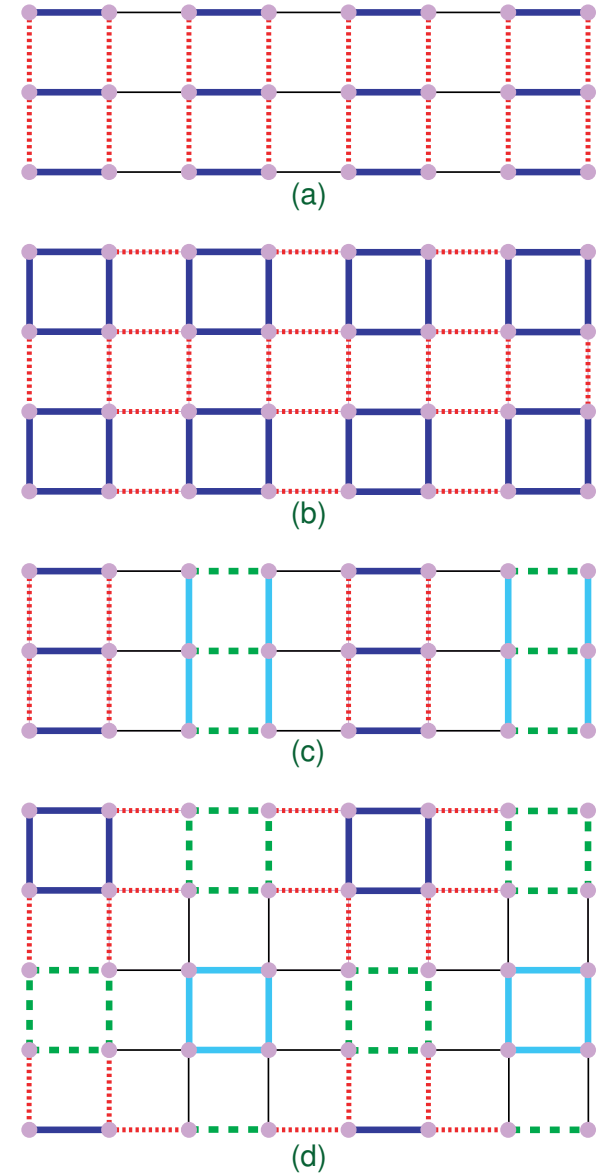


FIG. 6 Pattern of the bond variables $\langle Q_a(\vec{r}_j) \rangle$, for \vec{r}_a a nearest-neighbor vector, in a number of paramagnetic states with $\langle \mathbf{S}_j \rangle = 0$. For each state, the values of $\langle Q_a(\vec{r}_j) \rangle$ are equal on bonds represented by the same type of line, and unequal otherwise. The number of distinct values of $\langle Q_a(\vec{r}_j) \rangle$ are (a) 3, (b) 2, (c) 5, and (d) 5. The unit cells of the ground states have sizes (a) 2×1 , (b) 2×2 , (c) 4×1 , and (d) 4×4 .

a measure of the charge density⁵ on site \vec{r}_j , and so this special case of (10) measures the “charge order.”

The state introduced in Fig 5 can be characterized by the pattern of values of $\langle Q_a(\vec{r}_j) \rangle$ with \vec{r}_a a nearest neighbor vector.

⁵ By (10), $Q_0(\vec{r}_j) = \mathbf{S}_j^2$. A site with a spin has $\mathbf{S}_j^2 = 3/4$, while a site with a hole has $\mathbf{S}_j^2 = 0$, and we assume that doubly occupied sites are very rare. Thus \mathbf{S}_j^2 , and hence $Q_a(\vec{r}_j)$ is seen to be linearly related to the charge density on site j .

bor vector, as shown in Fig 6a: notice there are 3 distinct values of $\langle Q_a(\vec{r}_j) \rangle$ and symmetries of the states in Figs 5 and 6a are identical. While these 3 values are quite different in the trial state in Fig 5, their values in the actual ground state may be quite close to each other: it is only required that they not be exactly equal.

Another closely related bond-ordered state, which has appeared in some theories (Altman and Auerbach, 2002; Dombre and Kotliar, 1989; Read and Sachdev, 1989a; Sachdev and Read, 1996), is shown in Fig 6b: here the bonds have a plaquette-like arrangement rather than columnar, but, as we shall discuss below, the physical properties of all the states in Fig 6 are quite similar to each other.

We can also consider patterns of bond order with larger unit cells, and two important structures which have appeared in theories of doped Mott insulators (Vojta, 2002; Vojta and Sachdev, 1999) are shown in Figs 6c and 6d (related bond orders also appear in studies of quasi-one-dimensional models appropriate to organic superconductors (Clay *et al.*, 2002; Mazumdar *et al.*, 2000)). Again, as in Section III.A.1, such states could, in principle, also appear in Mott insulators with longer-range exchange in (5). An interesting property of these states is that, unlike the states in Fig 6a and 6b, not all sites are crystallographically equivalent. This means that on-site spin-singlet observables, such as the site charge density, will also have a spatial modulation from site to site. A subtlety is that the Hamiltonian (5) acts on a Hilbert space of $S = 1/2$ spins on every site, and so the charge density on each site is fixed at unity. However, it must be remembered that (5) is an effective model derived from an underlying Hamiltonian which does allow virtual charge fluctuations, and the site charge modulations in the states of Figs 6c and 6d will appear when it is properly computed in terms of the microscopic degrees of freedom. At the same time, this argument also makes it clear that any such modulation is suppressed by the repulsive Coulomb energy, and could well be difficult to observe, even in the doped antiferromagnet. So the on-site variable, $\langle Q_0(\vec{r}_j) \rangle = \langle \mathbf{S}_j^2 \rangle$, will have a weak modulation in the states of Fig 6c and 6d when computed in the full Hilbert space of the model with charge fluctuations. Note, however, that the modulation in bond orders associated with $Q_a(\vec{r}_j)$, with $\vec{r}_a \neq 0$, need not be small in the states in Fig 6, as such modulations are not suppressed as effectively by the Coulomb interactions.

The physical mechanism inducing bond-ordered states such as those in Fig 6 is illustrated in the cartoon pictures in Fig 7. More detailed computations rely on a semiclassical theory of quantum fluctuations near a magnetically ordered state (Read and Sachdev, 1990). Remarkably, very closely related theories also appear from a very different starting point—from duality mappings (Fradkin and Kivelson, 1990; Read and Sachdev, 1990) of “quantum dimer models” (Rokhsar and Kivelson, 1988) of the paramagnetic state. These computations show that spontaneous bond order invariably appears in the

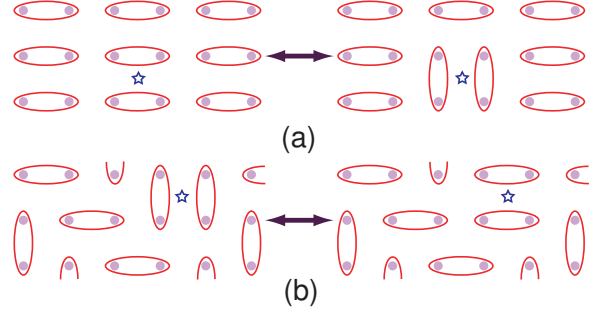


FIG. 7 Bond order induced by quantum fluctuations. Valence bonds gain energy by “resonating” in pairs (Anderson, 1987; Fazekas and Anderson, 1974; Pauling, 1949; Rokhsar and Kivelson, 1988); shown are resonances around the plaquette marked with a star. For the regular bond-ordered configuration of valence bonds in (a), such resonance can occur not only around the plaquette marked with a star, but around five additional plaquettes. In contrast, in (b), such a resonance is possible only around the plaquette marked with a star. This additional quantum “entropy” associated with (a) selects regular bond order in the ground state. More sophisticated considerations (which also allow valence bonds that do not connect nearest neighbor sites) show that this mechanism is especially effective in two dimensions (Read and Sachdev, 1990; Sachdev and Park, 2002).

ground state in systems with collinear spin correlations in two spatial dimensions (Read and Sachdev, 1990; Sachdev and Park, 2002). We will have more to say about this connection between bond and collinear spin order in Section III.C.1.

We also mention here the “nematic” states of Kivelson *et al.* (1998) in the doped Mott insulator. These can also be characterized by the bond order variables in (10). The symmetry of translations with respect to \vec{r}_j is not broken in such states, but the values of $\langle Q_a(\vec{r}_j) \rangle$ for symmetry-related values of \vec{r}_a become unequal. For example, $\langle Q_a(\vec{r}_j) \rangle$ has distinct values for $\vec{r}_a = (1, 0)$ and $(0, 1)$. Such states also appear in certain insulating antiferromagnets (Read and Sachdev, 1989a,b, 1990).

It is also interesting to note here that the bond order variables $Q_a(\vec{r}_j)$ also have spatial modulations in some of the magnetically ordered states considered in Section III.A (Zachar *et al.*, 1998). It is clear from (10) that any broken lattice symmetry in the spin-rotation invariant quantity $\langle \mathbf{S}_j \cdot \langle \mathbf{S}_{j+a} \rangle \rangle$ will generate a corresponding broken symmetry in the bond variable $\langle Q_a(\vec{r}_j) \rangle$. Evaluating the former using (6) we can deduce the following: (i) the $\vec{K} = (\pi, \pi)$ state in Fig 3a and the spiral state in Fig 4 have $\langle Q_a(\vec{r}_j) \rangle$ independent of \vec{r}_j , and hence no bond order; (ii) the bond-centered magnetically ordered state in Fig 3c has precisely the same pattern of bond order as the paramagnetic state in Fig 6c; (iii) the site-centered magnetically ordered state in Fig 3b has bond order with $\langle Q_a(\vec{r}_j) \rangle$ \vec{r}_j -dependent, but with a pattern distinct from any shown here—this pattern of bond order is in principle also allowed for paramagnetic states, but has so far not

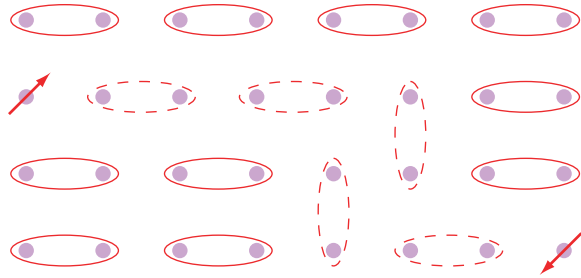


FIG. 8 Linear confining potential between two neutral $S = 1/2$ spinons in a bond-ordered state. The line of valence bonds with dashed lines is out of alignment with the global bond order, and it costs a finite energy per unit length.

been found to be stable in various studies. Finally, note that in (ii) and (iii) the period of the bond order (four) is half that of the spin modulation (eight)—this is easily seen to be a general relationship following from the correspondence $\langle Q_a(\vec{r}_j) \rangle \sim \langle \mathbf{S}_j \rangle \cdot \langle \mathbf{S}_{j+a} \rangle + \dots$ in magnetically ordered states, which with (6) implies an \vec{r}_j -dependent modulation of the bond order with wavevector $2\vec{K}$. It is worth reiterating here that this last relationship should not be taken to imply that there are no modulations in $\langle Q_a(\vec{r}_j) \rangle$ when $\langle \mathbf{S}_a \rangle = 0$: there can indeed be bond modulations in a paramagnet, as discussed in the other paragraphs of this subsection, and as is already clear from the simple wavefunction in Fig 5—these will be important later for physical applications.

We continue our exposition of paramagnetic bond-ordered states by describing excitations with non-zero spin. These can be understood simply by the analog of cartoon wavefunction pictures drawn in Fig 5. To create free spins we have to break at least one valence bond, and this initially creates two unpaired, neutral, $S = 1/2$ degrees of freedom (the “spinons”). We can ask if the spinons can be moved away from each other out to infinity, thus creating two neutral $S = 1/2$ quasiparticle excitations. As illustrated in Fig 8, this is not the case: connecting the two spinons is a line of defect valence bonds which is not properly aligned with the global bond order, and these defects have a finite energy cost per unit length. This linearly increasing potential is quite analogous to that between a quark and an anti-quark in a meson, and the spinons (quarks) are therefore permanently confined (Read and Sachdev, 1989b). Moving two spinons apart from each other will eventually force the breaking of the defect line by the creation of another pair of spinons. The only stable excitation with nonzero spin therefore consists of a pair of spinons and carries spin $S = 1$. We will refer to this quasiparticle as a *spin exciton* as its quantum numbers and observable characteristics are quite similar to spin excitons found in semiconductors and metals. The spin exciton is clearly the analog of a meson consisting of a quark and anti-quark pair.

A similar reasoning can be used to understand the influence of static spinless impurities *i.e.* the consequences

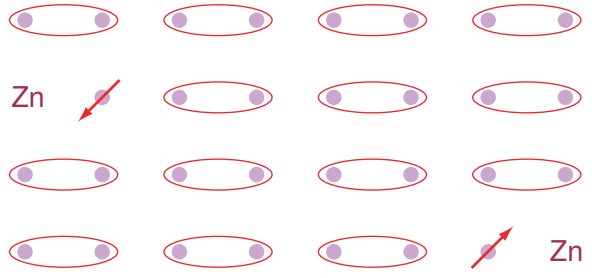


FIG. 9 Cartoon wavefunction for 2 static spinless Zn impurities in a confining, bond-ordered state. If we attempt to construct a wavefunction only using singlet valence bonds, then just as in Fig 8, there will be defect line of singlet bonds which are not aligned with the global bond order, which will cost a finite energy per unit length. When the two Zn impurities are sufficiently far apart, it will pay to restore the bond order in between the impurities, at the price of unpaired $S = 1/2$ moments, one near each impurity.

of removing a $S = 1/2$ spin from a fixed site j in (5). Experimentally, this can be conveniently done by substituting a spinless Zn^{++} ion in place of an $S = 1/2$ Cu ion. The main physical effect can be understood from the cartoon wavefunction in Fig 9: it is convenient to imagine placing 2 Zn impurities, and then moving them apart out to infinity to deduce the physics in the vicinity of a single impurity. As in our discussion above for spinons, note that there will initially be a line of defect valence bonds connecting the two Zn impurities, but it will eventually pay to annihilate this defect line by creating two spinons and binding each to a Zn impurity. Thus each Zn impurity *confines* a free $S = 1/2$ spinon in its vicinity, and this can be detected in experiments (Finkelstein *et al.*, 1990).⁶

2. Topological order: free spinons

This type of paramagnet is the “resonating valence bond” (RVB) state (Anderson, 1987; Baskaran and Anderson, 1988; Fazekas and Anderson, 1974; Kivelson *et al.*, 1987; Moessner and Sondhi, 2001; Pauling, 1949) in which the singlet pairings fluctuate in a liquid-like configuration,⁷ in contrast to the crystalline arrangement in

⁶ In principle the Zn impurity could also bind an electron (with or without a spinon) but this is suppressed by the charge gap in a Mott insulator. Later, in Section IV.C when we consider Zn impurities in d -wave superconductors, a related phenomenon appears in the form of the Kondo effect.

⁷ In recent years, Anderson (2002) has extended the RVB concept to apply to doped Mott insulators at temperatures *above* T_c . This extension is not in consonance with the classification of the present article. The topological order discussed in this subsection can only be defined at $T = 0$ in two spatial dimensions. The description at $T > T_c$ requires solution of a problem of quantitative difficulty, and with incoherent excitations, but without sharp distinctions between different states.

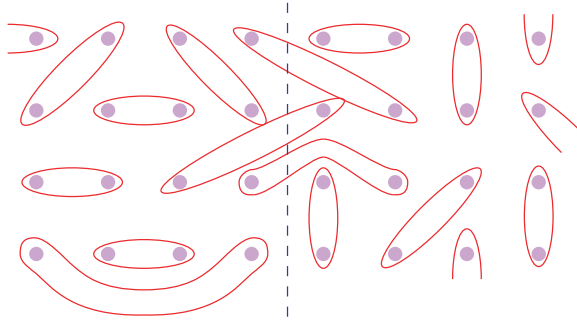


FIG. 10 Topological order in a resonating valence bond state. Shown is one component of the wavefunction, with a particular pairing of the spins into local singlets: the actual wavefunction is a superposition over a very large number of such pairing configurations. The number of valence bonds cutting the dashed line is an invariant modulo 2 over these pairing configurations, as shown by the following simple argument. Any rearrangement of the valence bonds can be reached by repeated application of an elementary rearrangement between 4 spins: $(1, 2)(3, 4) \rightarrow (1, 3)(2, 4)$ (here (i, j) denotes a singlet bond between \mathbf{S}_i and \mathbf{S}_j). So it is sufficient to check this conservation law for 4 spins: this is done easily by explicitly considering all different possibilities among spins 1, 2, 3, 4 residing to the left/right of the dashed line. If the system has periodic boundary conditions along the horizontal direction, then this conservation law is violated, but only by rearrangements associated with loops which circumnavigate the system; these only occur with a probability which becomes exponentially small as the circumference of the system increases.

Fig 5. Despite the apparent ‘disorder’ in the valence bond configuration in the ground state, there is actually a subtle topological order parameter which characterizes this type of Mott insulator (Bonesteel, 1989; Kivelson, 1989; Read and Chakraborty, 1989; Read and Sachdev, 1991; Rokhsar and Kivelson, 1988; Thouless, 1987; Wen, 1991), and which plays an important role in determining its excitation spectrum. The reader can see this in the context of the cartoon picture shown in Fig 10. Count the number of singlet valence bonds cutting the dashed line in this figure: this number will clearly depend upon the particular valence bond configuration chosen from the many present in the ground state, and one such is shown in Fig 10. However, as argued in the figure caption, the number of bonds cutting the dashed line is conserved modulo 2 between any two configurations which differ only local rearrangements of valence bonds: the quantum number associated with this conservation is the topological order in the ground state.

A convenient and powerful description of this topological order is provided by an effective model of the singlet sector formulated as Z_2 gauge theory (Read and Sachdev, 1991; Sachdev and Read, 1991; Senthil and Fisher, 2000; Wen, 1991).⁸ We postpone a self-contained derivation

of this Z_2 gauge theory to Section III.C.2 (see especially Fig 11): here, we show that such a gauge theory has similar topological properties. In a system with periodic boundary conditions (with the topology of a torus), the Z_2 gauge theory has different sectors depending upon whether there is a Z_2 flux piercing any of the holes of the torus (following Senthil and Fisher (2000), this Z_2 flux is now commonly referred to as a ‘vison’). In the valence bond picture discussed in the previous paragraph, a vison changes the sign associated with every valence bond cutting a line traversing the system in the vison direction (the dashed line in Fig 9); in other words, the even and odd valence bond sectors mentioned above now have their relative signs in the wavefunction changed.

In addition to appearing in the holes of the torus, the vison can also appear as a singlet excitation within the bulk (Kivelson, 1989; Read and Chakraborty, 1989; Read and Sachdev, 1991; Senthil and Fisher, 2000). It is now a vortex excitation in the Z_2 gauge theory, that requires a finite energy for its creation. We will see below in Section III.C.2 that there is an alternative, and physically revealing, interpretation of this vortex excitation in terms of the order parameters used earlier to characterize the magnetically ordered state, and that the topological order is intimately connected to the vison energy gap.

Finally, we can describe the spin-carrying excitations of this topologically ordered state using the crude, but instructive, methods used in Section III.B.1. As there is no particular bond order associated with the ground state, the spinons have no confining force between them, and are perfectly free to travel throughout the system as independent neutral $S = 1/2$ quasiparticles. Similarly, there is no confining force between Zn impurities and the spinons, and so it is not required that an $S = 1/2$ moment be present near each Zn impurity (Fendley *et al.*, 2002; Sachdev and Vojta, 2000).

C. Connections between magnetically ordered and paramagnetic states

A central ingredient in the reasoning of this article is the claim that there is an intimate connection between the magnetically ordered states in Section III.A and a corresponding paramagnetic state in Section III.B. In particular, the collinear states of Section III.A.1 are linked to the bond-ordered states in Section III.B.1, while

them by analogy to electromagnetism. The latter is a $U(1)$ gauge theory in which the physics is invariant under the transformation $z \rightarrow e^{i\phi}z$, $A_\mu \rightarrow A_\mu - \partial_\mu\phi$ where z is some matter field, A_μ is a gauge field, and ϕ is an arbitrary spacetime-dependent field which generates the gauge transformation. Similarly, in a Z_2 gauge theory, matter fields transform as $z \rightarrow \eta z$, where η is a spacetime-dependent field which generates the gauge transformation, but is now allowed to take only the values $\eta = \pm 1$. The Z_2 gauge field σ_{ij} resides on the links of a lattice, and transforms as $\sigma_{ij} \rightarrow \eta_i \sigma_{ij} \eta_j$.

⁸ Readers not familiar with Z_2 gauge theories may understand

the non-collinear states of Section III.A.2 are linked to the topologically ordered states of Section III.B.2. The reader will find a more technical discussion of the following issues in a companion review article by the author (Sachdev, 2003).

Before describing these links in the following subsections, we discuss the meaning of the “connectedness” of two states. The magnetically ordered phases are characterized by simple order parameters that we have discussed in Section III.A. Now imagine a second-order quantum phase transition in which the magnetic long-range order is lost, and we reach a state with fluctuating magnetic correlations, which is ultimately a rotationally invariant, spin-singlet paramagnet at the longest length scales. We will review arguments below which show that this “quantum disordered” state (Chakravarty *et al.*, 1989) is characterized by the order parameter of the connected paramagnetic state *i.e.* fluctuating collinear magnetic order leads to bond order, while fluctuating non-collinear magnetic order can lead to topological order. So two connected states are generically proximate to each other, without an intervening first order transition, in a generalized phase diagram drawn as a function of the couplings present in the Hamiltonian.

1. Collinear spins and bond order

It should be clear from Section III.A.1 that collinear spin states are characterized by a single vector \mathbf{N}_1 . The second vector \mathbf{N}_2 is pinned to a value parallel to \mathbf{N}_1 by some short distance physics, and at long distances we may consider a theory of the fluctuations of \mathbf{N}_1 alone. In a phase with magnetic order, the dominant spin-wave fluctuations occur in configurations with a fixed non-zero value of $|\mathbf{N}_1|$. In the transition to a non-magnetic phase, the mean value of $|\mathbf{N}_1|$ will decrease, until the fluctuations of \mathbf{N}_1 occur about $\mathbf{N}_1 = 0$ in a paramagnetic phase. There are 3 normal modes in this fluctuation spectrum, corresponding to the 3 directions in spin space, and the resultant is an $S = 1$ gapped quasiparticle excitation in the paramagnetic state. This we can easily identify as the $S = 1$ spin exciton of the bond-ordered state: this identification is evidence supporting our claimed connection between the states of Section III.A.1 and III.B.1.

Further evidence is provided by detailed computations which show the appearance of bond order in the regime where \mathbf{N}_1 fluctuations have lost their long-range order. We have already seen a simple example of this above in that the magnetically ordered state in Fig 3c already had the bond order of the paramagnetic state in Fig 6c: it is completely natural for the bond order in the magnetically ordered phase in Fig 3c to persist across a transition in which spin rotation invariance is restored, and this connects it to the state in Fig 6c. A non-trivial example of a related connection is that between the $\vec{K} = (\pi, \pi)$ Néel state in Fig 3a, and the paramagnetic bond-ordered states in Figs 6a and 6b, which was established by Read

and Sachdev (1989b), Read and Sachdev (1990), and Sachdev and Park (2002): Berry phases associated with the precession of the lattice spins were shown, after a duality mapping, to induce bond order in the phase in which long-range order in \mathbf{N}_1 was lost.

2. Non-collinear spins and topological order

The first argument of Section III.C.1, when generalized to non-collinear spins, leads quite simply to a surprisingly subtle characterization of the associated paramagnetic phase.

Recall from Section III.A.2 that the non-collinear magnetic phase is characterized by two orthogonal, and equal length, vectors $\mathbf{N}_{1,2}$. It takes 6 real numbers to specify two vectors, but the 2 constraints in (7) reduce the number of real parameters required to specify the ordered state to 4. There is a useful parameterization (Chubukov *et al.*, 1994b,c) which explicitly solves the constraints (7) by expressing $\mathbf{N}_{1,2}$ in terms of 2 complex numbers z_\uparrow, z_\downarrow (which are equivalent to the required 4 real numbers):

$$\mathbf{N}_1 + i\mathbf{N}_2 = \begin{pmatrix} z_\downarrow^2 - z_\uparrow^2 \\ i(z_\uparrow^2 + z_\downarrow^2) \\ 2z_\uparrow z_\downarrow \end{pmatrix} \quad (11)$$

It can also be checked from (11) that $(z_\uparrow, z_\downarrow)$ transforms like an $S = 1/2$ spinor under spin rotations. So instead of dealing with a constrained theory of $\mathbf{N}_{1,2}$ fluctuations, we can express the theory in terms of the complex spinor $(z_\uparrow, z_\downarrow)$, which is free of constraints. There is one crucial price we have to pay for this simplification: notice that the parametrization (11) is *double-valued* and that the spinors $(z_\uparrow, z_\downarrow)$ and $(-z_\uparrow, -z_\downarrow)$ both correspond to the same non-collinearly ordered state. Indeed, we can change the sign of z independently at different points in spacetime without changing the physics, and so any effective action for the $(z_\uparrow, z_\downarrow)$ spinor must be obey a Z_2 gauge invariance. Here is our first connection with the topologically ordered paramagnetic state of Section III.B.2, where we had also discussed a description by a Z_2 gauge theory.

In the magnetically ordered non-collinear state we expect dominant rotational fluctuations about some fixed non-zero value $\mathbf{N}_1^2 = \mathbf{N}_2^2 = (|z_\uparrow|^2 + |z_\downarrow|^2)^2$. The constraint $|z_\uparrow|^2 + |z_\downarrow|^2 = \text{constant}$ defines the surface of a sphere in a four-dimensional space (S_3) of magnetically ordered ground states defined by the real and imaginary components of z_\uparrow, z_\downarrow . However, we need to identify opposite points on the sphere with each other, as $(z_\uparrow, z_\downarrow)$ and $(-z_\uparrow, -z_\downarrow)$ are equivalent states: this identifies the order parameter space with S_3/Z_2 . This quotient form has crucial consequences for the topological defect excitations that are permitted in both the magnetically ordered and the paramagnetic phases. In particular, the order parameter space (see the review article by Mermin (1979)) allows stable Z_2 vortices associated with the first homotopy group $\pi_1(S_3/Z_2) = Z_2$: upon encircling such a

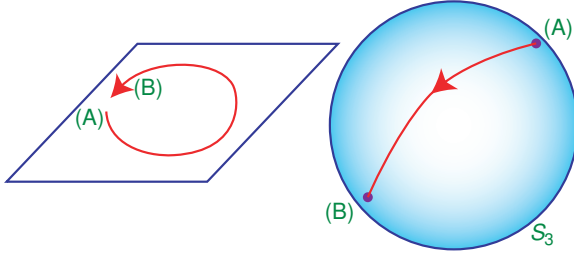


FIG. 11 A vison (Senthil and Fisher, 2000). On the left we show a circular path in real space; this path could be entirely within the bulk of the system (in which case it defines a local vison excitation) or it encircles the entire system, which obeys periodic boundary conditions (so that now it defines a global topological excitation). On the right is the space of magnetically ordered states represented by the complex spinor $(z_\uparrow, z_\downarrow)$ up to an overall sign. As we traverse the real space circle, the path in order parameter space connects polar opposite points on S_3 (A and B), which are physically indistinguishable. A key point is that this vison excitation can be defined even in a state in which magnetic order is lost: the path on the right will fluctuate all over the sphere in quantum imaginary time, as will the location of the points A and B, but A and B will remain polar opposites.

vortex, we traverse a path in the order parameter space from $(z_\uparrow, z_\downarrow)$ to $(-z_\uparrow, -z_\downarrow)$, as shown in Fig 11. As argued in the caption, a fundamental point is that such vortices can be defined as sensible excitations even in the paramagnetic phase, where $(z_\uparrow, z_\downarrow)$ is strongly fluctuating in quantum imaginary time: upon encircling the vortex, the path in order parameter space will also strongly fluctuate, but will always connect polar opposite points on S_3 . We identify these paramagnetic vortices with the vortons of Section III.B.2, thus firmly establishing a connection between non-collinear magnetic order and the topologically ordered paramagnet.

Finally, we wish to consider a Z_2 gauge theory in which magnetic order is lost continuously (Chubukov *et al.*, 1994c; Read and Sachdev, 1991), and we obtain a paramagnetic phase in which the spinor $(z_\uparrow, z_\downarrow)$ fluctuates about 0. A pedagogical description of such a theory was provided by Lammert *et al.* (1993) and Lammert *et al.* (1995) in an entirely different context: they considered thermal phase transitions in a nematic liquid crystal, with order parameter S_2/Z_2 , in three spatial dimensions. However their results can be transposed to the quantum phase transition in two spatial and one imaginary time dimension of interest here, with the primary change being in the order parameter space from S_2/Z_2 to S_3/Z_2 : this change is only expected to modify uninteresting numerical factors in the phase diagram, as the global topologies of the two spaces are the same. As shown by Lammert *et al.* (1993) and Lammert *et al.* (1995), the magnetically ordered state (with states labeled by points in $S_{2,3}/Z_2$) does indeed undergo a continuous phase transition to a paramagnetic state in which spin rotation invariance is restored and a topological order is present. This topo-

logical order arises because the Z_2 vortons discussed in Fig 11 do not proliferate in the paramagnetic state; in this sense, the topological order here is similar to the topological order in the low temperature phase of the classical XY model in 2 dimensions, where point vortices are suppressed below the Kosterlitz-Thouless transition (Thouless, 1998). We can also connect the nonproliferation of vortons to our discussion in Section III.B.2, where we noted that there was an excitation gap towards the creation of Z_2 vortons (Senthil and Fisher, 2000). Indeed, an explicit connection between the topological order being discussed here and the topological order noted in the caption to Fig 10 was established by Read and Sachdev (1991), Sachdev and Read (1991), and Chubukov *et al.* (1994c).

Moreover, without the proliferation of vortons in the ground state, the $(z_\uparrow, z_\downarrow)$ configurations can be defined as single-valued configurations throughout the sample. Normal-mode oscillations of $(z_\uparrow, z_\downarrow)$ about zero can now be identified as a neutral $S = 1/2$ particle. This is clearly related to the spinon excitation of Section III.B.2; this is our final confirmation of the intimate connection between the non-collinear magnetic states of Section III.A.2 and the topologically ordered states of Section III.B.2.

This is a good point to mention, in passing, recent neutron scattering evidence for a RVB state in Cs_2CuCl_4 (Coldea *et al.*, 2001); the measurements also show non-collinear spin correlations, consistent with the connections being drawn here.

IV. ORDER IN STATES PROXIMATE TO MOTT INSULATORS

We are now ready to discuss the central issue of order parameters characterizing the cuprate superconductors. These superconductors are obtained by introducing mobile charge carriers into the Mott insulator of the square lattice of Cu ions that was discussed at the beginning of Section III. The charge carriers are introduced by substitutional doping. For instance, in the compound $\text{La}_{2-\delta}\text{Sr}_\delta\text{CuO}_4$, each trivalent La^{3+} ion replaced by a divalent Sr^{2+} ion causes one hole to appear in the Mott insulator of Cu ions: the concentration of these holes is δ per square lattice site.

For large enough δ , theory and experiment both indicate that such a doped Mott insulator is a d -wave superconductor characterized by the pairing amplitude (2). The reader can gain an intuitive (but quite crude and incomplete) understanding of this by the similarity between the real-space, short-range pair in (9) and the momentum-space, long-range pairing in (2). The undoped Mott insulator already has electrons paired into singlet valence bonds, as in (9), but the repulsive Coulomb energy of the Mott insulator prevents motion of the charge associated with this pair of electrons. It should be clear from our discussion in Section III.B that this singlet pairing is complete in the paramagnetic Mott

insulators, but we can also expect a partial pairing in the magnetically ordered states. Upon introducing holes into the Mott insulator, it becomes possible to move charges around without any additional Coulomb energy cost, and so the static valence bond pairs in (9) transmute into the mobile Cooper pairs in (2); the condensation of these pairs leads to superconductivity. Note that this discussion is concerned with the nature of the ground state wavefunction, and we are not implying a “mechanism” for the formation of Cooper pairs.

The discussion in the previous sections has laid the groundwork for a more precise characterization of this superconductor using the correlations of various order parameters, and of their interplay with each other. The proximity of the Mott insulator indicates that the Cooper pairs should be considered descendants of the real-space, short range pairs in (9), and this clearly demands that all the magnetic, bond and topological order parameters discussed in Section III remain viable candidates for the doped Mott insulator. The motion of charge carriers allows for additional order parameters, and the most important of these is clearly the superconducting order of the BCS state noted below (2) in Section II. In principle, it is also possible to obtain new order parameters which are characteristic of *neither* the BCS state *nor* a Mott insulator, but we such order parameters shall not be discussed here (discussions of one such order may be found in Hsu *et al.* (1991), Wen and Lee (1996), Lee and Sha (2003), Chakravarty *et al.* (2001), and Schollwöck *et al.* (2002)).

The arsenal of order parameters associated with Mott insulators and the BCS state permits a very wide variety of possible phases of doped Mott insulators, and of quantum phase transitions between them. Further progress requires experimental guidance, but we claim that valuable input is also obtained from the theoretical connections sketched in Section III.C.

The simplest line of reasoning (Sachdev and Read, 1991) uses the fact that the undoped Mott insulator La_2CuO_4 has collinear magnetic order as sketched in Fig 3a. The arguments above and those in Section III.C then imply that the doped Mott insulator should be characterized by the collinear magnetic order of Section III.A.1, the bond order of Section III.B.1, along with the phase order of BCS theory. This still permits a large variety of phase diagrams, and some of these were explored in Sachdev and Read (1991), Vojta and Sachdev (1999), Vojta *et al.* (2000a), and Vojta (2002), with detailed results on the evolution of bond order and superconductivity with increasing doping. However, this reasoning excludes phases associated with the non-collinear magnetic order of Section III.A.2 and the topological order of Section III.B.2.

Some support for this line of reasoning came from the breakthrough experiments of Tranquada *et al.* (1995), Tranquada *et al.* (1996), and Tranquada *et al.* (1997) on $\text{La}_{2-y-\delta}\text{Nd}_y\text{Sr}_\delta\text{O}_4$ for hole concentrations near $\delta = 1/8$: they observed static, collinear magnetic order near the

wavevectors $\vec{K} = (3\pi/4, \pi)$ shown in Figs 3b,c, which co-existed microscopically⁹ with superconductivity for most δ . They also observed modulations in the bond order $Q_a(\vec{r}_j)$ (Eqn (10)) at the expected wavevector, $2\vec{K}$. The experimentalists interpreted their observations in terms of modulations of the site charge density—proportional to $Q_0(\vec{r}_j)$ —but the existing data actually do not discriminate between the different possible values of \vec{r}_a . As we noted earlier in Section III.B.1, the physical considerations of the present article suggest that the modulation may be stronger with $\vec{r}_a \neq 0$. (The existing data also cannot distinguish between the magnetic orders in Fig 3b (site-centered) and Fig 3c (bond-centered), or between the bond orders in Fig 6c (orthorhombic symmetry) and Fig 6d (tetragonal symmetry).) We also mention here the different physical considerations in the early theoretical work of Zaanen and Gunnarsson (1989), Machida (1989), Schulz (1989), and Poilblanc and Rice (1989) which led to insulating states with collinear magnetic order with wavevector $\vec{K} \neq (\pi, \pi)$ driven by a large site-charge density modulation in the domain walls of holes.

The following subsections discuss a number of recent experiments which explore the interplay between the order parameters we have introduced here. We argue that all of these experiments support the proposal that the cuprate superconductors are characterized by interplay between the collinear magnetic order of Section III.A.1, the bond order of Section III.B.1 (these are connected as discussed in Section III.C.1), and the superconducting order of BCS theory.

A. Tuning order by means of a magnetic field

In Section I, we identified a valuable theoretical tool for the study of systems with multiple order parameters: use a coupling g to tune the relative weights of static or fluctuating order parameter correlations in the ground state. Is such a coupling available experimentally? One choice is the hole concentration, δ , and we can assume here that g increases monotonically with δ . However, δ is often difficult to vary continuously, and it may be that sampling the phase diagram along this one-dimensional axis may not reveal the full range of physically relevant behavior. A second tuning parameter will be clearly valuable; here we argue that, under suitable conditions, this is provided by a magnetic field applied perpendicular to the two-dimensional layers.

Consider the case where both phases in Fig 1 are superconducting; the phase with $g < g_c$ then has co-existence of long-range order in superconductivity and a secondary order parameter. We also restrict attention to the case

⁹ The microscopic co-existence of magnetic order and superconductivity is not universally accepted, but strong arguments in its favor have been made recently by Khaykovich *et al.* (2002).

where the transition at $g = g_c$ is second order (related results apply also to first order transitions, but we do not discuss them here). Imposing a magnetic field, H , on these states will induce an inhomogeneous state, consisting of a lattice of vortices surrounded by halos of superflow (we assume here that $H > H_{c1}$, the lower critical field for flux penetration). In principle, we now need to study the secondary order parameter in this inhomogeneous background, which can be a problem of some complexity. However, it was argued by Demler *et al.* (2001) and Zhang *et al.* (2002) that the problem simplifies considerably near the phase boundary at $g = g_c$. Because of the diverging correlation length associated with the secondary order parameter, we need only look at the spatially-averaged energy associated with the relevant order parameters. We know from the standard theory of the vortex lattice in a BCS superconductor (Parks, 1969) that the energy density of the superconducting order increases by the fraction $\sim (H/H_{c2}) \ln(H_{c2}/H)$, where $H_{c2} \gg H_{c1}$ is the upper critical field above which superconductivity is destroyed. Let us make the simple assumption that this change in energy of the superconducting order can also be characterized by a change in the coupling constant g . We can therefore introduce an effective coupling $g_{\text{eff}}(H)$ given by

$$g_{\text{eff}}(H) = g - C' \left(\frac{H}{H_{c2}} \right) \ln \left(\frac{H_{c2}}{H} \right) \quad (12)$$

where C' is some constant of order unity. As g is linearly related to δ , we can also rewrite this expression in terms of an effective doping concentration $\delta_{\text{eff}}(H)$,

$$\delta_{\text{eff}}(H) = \delta - C \left(\frac{H}{H_{c2}} \right) \ln \left(\frac{H_{c2}}{H} \right), \quad (13)$$

where C is some other constant. These expressions imply that we tune through different values of g or δ simply by varying the applied magnetic field.

The sign of C is of some physical importance, and can be deduced by a simple argument. It is observed that in the lightly doped cuprates, decreasing δ leads to a stabilization of an order associated with the Mott insulator at the expense of the superconducting order. (There is a non-monotonic dependence on δ from commensurability effects near $\delta = 1/8$, but here too the magnetic order is stabilized at the expense of superconductivity). As increasing H clearly suppresses the superconducting order, it must be the case that $\delta_{\text{eff}}(H)$ decreases with increasing H . This implies that $C > 0$, and indicates a competition (Tranquada *et al.*, 1997) between the two ground states, or order parameters, on either side of the quantum critical point (Chubukov *et al.*, 1994a; Sachdev, 2000; Zhang, 1997).

The relationships (12) and (13) can be combined with Fig 1 to produce a phase diagram in the (g, H) (or (δ, H)) plane. This is shown in Fig 12. Notice that the phase boundary comes into the $g = g_c, H = 0$ point with vanishing slope. This implies that a relatively small field is

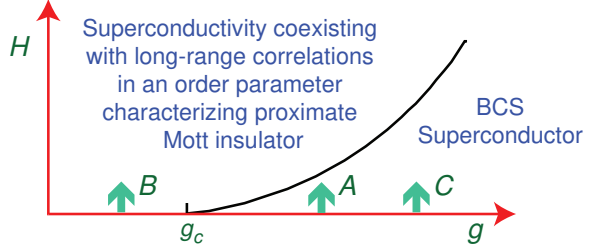


FIG. 12 Phase diagram in the g, H plane deduced from (12). The phase boundary is determined by setting $g_{\text{eff}}(H) = g_c$, which leads to a phase boundary at a critical field $H \sim (g - g_c)/\ln(1/(g - g_c))$. We assume that g is a monotonically increasing function of δ . The collinear magnetic order of Figs 3b and c is the secondary order parameter investigated in recent neutron scattering experiments in doped La_2CuO_4 : the observations of Lake *et al.* (2001) are along the arrow A, and those of Katano *et al.* (2000), Lake *et al.* (2002), Khaykovich *et al.* (2002), and Khaykovich *et al.* (2003) are along the arrow B. The STM experiments of Hoffman *et al.* (2002a), Hoffman *et al.* (2002b), Howald *et al.* (2002), Howald *et al.* (2003) are along arrow C, and will be discussed in Section IV.D.

needed in the $g > g_c$ region to tune a BCS superconductor across a quantum phase transition into a state with long-range correlations in the secondary order parameter. There are also some interesting modifications to Fig 12 in the fully three-dimensional model which accounts for the coupling between adjacent CuO_2 layers; these are discussed by Kivelson *et al.* (2002b).

A number of neutron scattering studies of the physics of Fig 12 in doped La_2CuO_4 have recently appeared. The secondary order parameter here is the collinear magnetic order of Figs 3b and c, which is also observed in $\text{La}_{2-y-\delta}\text{Nd}_y\text{Sr}_\delta\text{O}_4$ as discussed above. Earlier, a series of beautiful experiments by Wakimoto *et al.* (1999), Lee *et al.* (1999), and Wakimoto *et al.* (2001) established that $\text{La}_{2-\delta}\text{Sr}_\delta\text{CuO}_4$ has long-range, collinear magnetic order co-existing with superconductivity for a range of δ values above $\delta = 0.055$. Moreover, the anomalous frequency and temperature dependence of the dynamic spin structure factor (Chubukov *et al.*, 1994a; Sachdev and Ye, 1992) in neutron scattering experiments by Aeppli *et al.* (1997) gave strong indications of a second-order quantum phase transition near $\delta \approx 0.14$ at which the magnetic order vanished. We identify this transition with the point $g = g_c, H = 0$ in Fig 12. Recent studies have explored the region with $H > 0$: Lake *et al.* (2001) observed a softening of a collective spin excitation mode at $\delta = 0.163$ in the presence of an applied magnetic field. We interpret this as a consequence of the low H approach to the phase boundary in Fig 12 in the $g > g_c$ region, as indicated by the arrow labeled A. Notice that the field was not large enough to cross the phase boundary.

A separate set of experiments have examined the H dependence of the static magnetic moment in the superconductor with $g < g_c$ in $\text{La}_{2-\delta}\text{Sr}_\delta\text{CuO}_4$ (Katano *et al.*, 2000; Lake *et al.*, 2002) and $\text{La}_2\text{CuO}_{4+y}$ (Khaykovich

et al., 2003, 2002), along the arrow indicated by B in Fig 12. The theoretical prediction (Demler *et al.*, 2001; Zhang *et al.*, 2002) for these experiments is a simple consequence of (12) and (13). Let $I(H, \delta)$ be the observed intensity of the static magnetic moment associated with the order in Figs 3b,c at a field H and doping δ . If we assume that the dominant effect of the field can be absorbed by replacing δ by the effective $\delta_{\text{eff}}(H)$, we can write

$$\begin{aligned} I(H, \delta) &\approx I(H = 0, \delta_{\text{eff}}(H)) \\ &\approx I(H = 0, \delta) + \mathcal{D} \left(\frac{H}{H_{c2}} \right) \ln \left(\frac{H_{c2}}{H} \right), \end{aligned} \quad (14)$$

where in the second expression we have used (13) and expanded in powers of the second argument of I . Reasoning as in the text below (13) for \mathcal{C} , we use the experimental fact that a decrease in δ leads to an increase in the magnetic order, and hence $\mathcal{D} > 0$. The results of recent experiments (Khaykovich *et al.*, 2003, 2002; Lake *et al.*, 2002) are in good agreement with the prediction (14), with a reasonable value for \mathcal{D} obtained by fitting (14) to the experimental data.

B. Detecting topological order

The magnetic and bond orders break simple symmetries of the Hamiltonian, and, at least in principle, these can be detected by measurement of the appropriate two-point correlation function in a scattering experiment. The topological order of Sections III.B.2 and III.C.2 is a far more subtle characterization of the electron wavefunction, and can only be observed indirectly through its consequences for the low energy excitations. We review here the rationale behind some recent experimental searches (Bonn *et al.*, 2001; Wynn *et al.*, 2001) for topological order.

The searches relied on a peculiar property of a superconductor proximate to a Mott insulator with topological order: there is a fundamental distinction in the internal structure of vortices in the superconducting order, specified by (3), which depends on whether the integer n_v is even or odd. This difference was noted (Nagaosa and Lee, 1992; Sachdev, 1992) in the context of a simple mean-field theory of a superconductor near an insulating spin gap state. However, the significance and interpretation of the mean-field result, and in particular its connection with topological order, did not become apparent until the far-reaching work of Senthil and Fisher (2000), Senthil and Fisher (2001a), and Senthil and Fisher (2001b). The arguments behind the dependence on the parity of n_v are subtle, and only an outline will be sketched here—the reader is referred to Senthil and Fisher (2001a) and Senthil and Fisher (2001b) for a complete exposition. Although the superconducting order of BCS theory in (2) and the topological order of the Mott insulator are quite distinct entities, there is an important connection between them in the superconducting state: each vortex

with n_v odd in (3) has a vison attached to it. The vison gap in the proximate Mott insulator then increases the energy required to create n_v odd vortices, while this extra energy is not required for n_v even.

The connection between n_v odd vortices and visons is most transparent for the case where the spinons in the Mott insulator obey fermionic statistics. We considered bosonic spinons z_σ in Section III.C.2, but they can transmute into fermions by binding with a vison (Demler *et al.*, 2002; Kivelson, 1989; Read and Chakraborty, 1989): we represent the fermionic spinon by $f_{j\sigma}$. In the doped Mott insulator, each electron annihilation operator, $c_{j\sigma}$, must create at least one neutral $S = 1/2$ spinon excitation, along with a charge e hole (Kivelson *et al.*, 1987), and we can represent this schematically by the operator relation

$$c_{j\sigma} = b_j^\dagger f_{j\sigma}, \quad (15)$$

where b_j^\dagger creates a bosonic spinless hole. In this picture of the doped Mott insulator, the presence of superconductivity as in (2) requires both the condensation of the b_j , along with the condensation of “Cooper pairs” of the spinons $f_{j\sigma}$. We can deduce this relationship from (2) and (15) which imply, schematically

$$\Delta_0 = \Delta_f b^2, \quad (16)$$

where we have ignored spatial dependence associated with the internal wavefunction of the Cooper pair (hence there are no site subscripts j in (16)), and $\Delta_f \sim \langle f_{j\uparrow} f_{j'\downarrow} \rangle$ is the spinon pairing amplitude. From (16) we see if the phase of b_j winds by 2π upon encircling some defect site, then phase of Δ_0 will wind by 4π , and this corresponds to a vortex in the superconducting order with $n_v = 2$ in (3). Indeed, the only way (16) can lead to an elementary vortex with $n_v = 1$ is if the phase of the spinon pair amplitude, Δ_f , winds by 2π upon encircling the vortex: the latter is another description of a vison (Senthil and Fisher, 2000). This argument is easily extended to show that every odd n_v vortex must be associated with at least an elementary vortex in the phase of Δ_f , thus establishing our claimed connection.

Sufficiently close to the Mott insulator, and near a second-order superconductor-insulator transition, the energy required to create a vison raises the energy of $n_v = 1$ vortices, and the lowest energy vortex lattice state in an applied magnetic field turns out to have vortices with flux hc/e , which is twice the elementary flux (Sachdev, 1992). This should be easily detectable, but such searches have not been successful so far (Wynn *et al.*, 2001).

More recently Senthil and Fisher (2001a) have proposed an ingenious test for the presence of visons, also relying on the binding of a vison to a vortex with flux $hc/(2e)$. Begin with a superconductor in a toroidal geometry with flux $hc/(2e)$ penetrating the hole of the torus. By the arguments above, a vison is also trapped in the hole of the torus. Now by changing either the temperature or the doping level of the superconductor, drive it into a normal state. This will allow the magnetic flux

to escape, but the topological order in the bulk will continue to trap the vison. Finally, return the system back to its superconducting state, and, quite remarkably, the vison will cause the magnetic flux to reappear. An experimental test for this “flux memory effect” has also been undertaken (Bonn *et al.*, 2001), but no such effect has yet been found.

So despite some innovative and valuable experimental tests, no topological order has been detected so far in the cuprate superconductors.

C. Non magnetic impurities

We noted in Section III.B.1 that one of the key consequences of the confinement of spinons in the bond-ordered paramagnet was that each non-magnetic impurity would bind a free $S = 1/2$ moment. In contrast, in the topologically ordered RVB states of Section III.B.2, such a moment is not generically expected, and it is more likely that the “liquid” of valence bonds would readjust itself to screen away the offending impurity without releasing any free spins.

Moving to the doped Mott insulator, we then expect no free $S = 1/2$ moment for the topologically ordered case. The remaining discussion here is for the confining case; in this situation the $S = 1/2$ moment may well survive over a finite range of doping, beyond that required for the onset of superconductivity. Eventually, at large enough hole concentrations, the low energy fermionic excitations in the d -wave superconductor will screen the moment (by the Kondo effect) at the lowest temperatures. However, unlike the case of a Fermi liquid, the linearly vanishing density of fermionic states at the Fermi level implies that the Kondo temperature can be strictly zero for a finite range of parameters (Gonzalez-Buxton and Ingersent, 1998; Vojta and Bulla, 2002; Withoff and Fradkin, 1990). So we expect each non-magnetic impurity to create a free $S = 1/2$ moment that survives down to $T = 0$ for a finite range of doping in a d -wave superconductor proximate to a confining Mott insulator. The collinear magnetic or bond order in the latter insulator may also survive into the superconducting state, but there is no fundamental reason for the disappearance of these long-range orders (bulk quantum phase transitions) to coincide with the zero temperature quenching of the moment (an impurity quantum phase transition).

A very large number of experimental studies of non-magnetic Zn and Li impurities have been carried out. Early on, in electron paramagnetic resonance experiments Finkelstein *et al.* (1990) observed the trapping of an $S = 1/2$ moment near a Zn impurity above the superconducting critical temperature, and also noted the implication of their observations for the confinement of spinons, in the spirit of our discussion above. Subsequent specific heat and nuclear magnetic resonance experiments (Alloul *et al.*, 1991; Bobroff *et al.*, 2001; Julien *et al.*, 2000; Sisson *et al.*, 2000) have also explored low temper-

atures in the superconducting state, and find evidence of spin moments, which are eventually quenched by the Kondo effect in the large doping regime. Especially notable is the recent nuclear magnetic resonance evidence (Bobroff *et al.*, 2001) for a transition from a $T = 0$ free moment state at low doping, to a Kondo quenched state at high doping.

We interpret these results as strong evidence for the presence of an $S = 1/2$ moment near non-magnetic impurities in the lightly doped cuprates. We have also argued here, and elsewhere (Sachdev and Vojta, 2000), that the physics of this moment formation is most naturally understood in terms of the physics of a proximate Mott insulator with spinon confinement.

The creation of a free magnetic moment (with a local magnetic susceptibility which diverges as $\sim 1/T$ as $T \rightarrow 0$) near a single impurity implies that the cuprate superconductors are exceptionally sensitive to disorder. Other defects, such as vacancies, dislocations, and grain boundaries, which are invariably present even in the best crystals, should also have similar strong effects. We speculate that it is this tendency to produce free moments (and local spin order which will be induced in their vicinity) which is responsible for the frequent recent observation of magnetic moments in the lightly doped cuprates (Sidis *et al.*, 2001; Sonier *et al.*, 2001).

D. STM studies of the vortex lattice

Section IV.A discussed the tuning of collinear magnetic order by means of an applied magnetic field, and its detection in neutron scattering experiments in doped La_2CuO_4 . This naturally raises the question of whether it may also be possible to detect the bond order of Section III.B.1 somewhere in the phase diagram of Fig 12. Clearly the state with co-existing collinear magnetic and superconducting order (explored by experiments along the arrow B) should, by the arguments of Section III.C.1, also have co-existing bond order. However, more interesting is the possibility that the BCS superconductor itself has local regions of bond order for $H \neq 0$ (Park and Sachdev, 2001). As we have argued, increasing H increases the weight of the Mott insulator order parameter correlations in the superconducting ground state. The appearance of static magnetic order requires breaking of spin rotation invariance (in the plane perpendicular to the applied field), and this cannot happen until there is a bulk phase transition indicated by the phase boundary in Fig 12. In contrast, bond order only breaks translational symmetry, but this is already broken by the vortex lattice induced by a non-zero H . The small vortex cores can pin the translational degree of freedom of the bond order, and a halo of static bond order should appear around each vortex core (Demler *et al.*, 2001; Park and Sachdev, 2001; Polkovnikov *et al.*, 2001, 2002b; Zhang *et al.*, 2002). Notice that this bond order has appeared in the state which has only superconducting order at $H = 0$,

and so should be visible along the arrow labelled C in Fig 12. Recall also our discussion in Section III.B.1 that site charge order is a special case of bond order (with $\vec{r}_a = 0$ in the bond order parameter $Q_a(\vec{r})$).

Many other proposals have also been made for additional order parameters within the vortex core. The earliest of these involved dynamic antiferromagnetism (Nagaosa and Lee, 1992; Sachdev, 1992), and were discussed in Section IV.B in the context of topological order. Others (Andersen *et al.*, 2002; Arovas *et al.*, 1997; Chen *et al.*, 2002; Chen and Ting, 2002; Franz *et al.*, 2002; Ghosal *et al.*, 2002; Ichioka and Machida, 2002; Zhang, 1997; Zhu *et al.*, 2002) involve static magnetism within each vortex core in the superconductor.¹⁰ This appears unlikely from the perspective of the physics of Fig 12, in which static magnetism only appears after there is a co-operative bulk transition to long-range magnetic order, in the region above the phase boundary; below the phase boundary there are no static “spins in vortices,” but there is bond order as discussed above (Park and Sachdev, 2001; Zhang *et al.*, 2002). (Static spins do appear in the three space dimensional model with spin anisotropy and inter-planar couplings considered in Kivelson *et al.* (2002b).) A separate proposal involving staggered current loops in the vortex core (Kishine *et al.*, 2001; Lee and Sha, 2003; Lee and Wen, 2001) has also been made.

Nanoscale studies looking for signals of bond order along the arrow C in Fig 12 would clearly be helpful. Scanning tunnelling microscopy (STM) is the ideal tool, but requires atomically clean surfaces of the cuprate crystal. The detection of collinear magnetic order in doped La_2CuO_4 makes such materials ideal candidates for bond order, but they have not been amenable to STM studies so far. Crystals of $\text{Bi}_2\text{Sr}_2\text{CaCu}_2\text{O}_{8+\delta}$ have been the focus of numerous STM studies, but there is little indication of magnetic order in neutron scattering studies of this superconductor. Nevertheless, by the reasoning in Fig 12, and using the reasonable hypothesis that a common picture of competing superconducting, bond, and collinear magnetic order applies to all the cuprates, it is plausible that static bond order should appear in $\text{Bi}_2\text{Sr}_2\text{CaCu}_2\text{O}_{8+\delta}$ for large enough H along the arrow C in Fig 12.

A number of atomic resolution STM studies of $\text{Bi}_2\text{Sr}_2\text{CaCu}_2\text{O}_{8+\delta}$ surfaces have appeared recently (Hoffman *et al.*, 2002a,b; Howald *et al.*, 2003, 2002). Hoffman *et al.* (2002a) observed a clear signal of modulations in the local density of electronic states, with a period of 4 lattice spacings, in a halo around each vortex core. There was no corresponding modulation in the surface topography, implying there is little modulation in the charge density. However, a bond order modulation, such as those in Figs 6c and d, could naturally lead to the required

modulation in the local density of states. Other studies (Hoffman *et al.*, 2002b; Howald *et al.*, 2003, 2002) have focused on the $H = 0$ region: here the modulations appear to have significant contributions (Byers *et al.*, 1993; Wang and Lee, 2003) from scattering of the fermionic $S = 1/2$ quasiparticles of the superconductor (Section II), but there are also signals (Howald *et al.*, 2003, 2002) of a weak residual periodic modulation in the density of states, similar to those found at $H \neq 0$. Theoretically (Howald *et al.*, 2003; Kivelson *et al.*, 2002a; Polkovnikov *et al.*, 2002a), it is quite natural that these quasiparticle and order parameter modulations co-exist. Howald *et al.* (2002) and Howald *et al.* (2003) also presented results for the energy dependence of this periodic modulation, and these appear to be best modelled by modulations in microscopic bond, rather than site, variables (Podolsky *et al.*, 2002; Vojta, 2002; Zhang, 2002).

This is a rapidly evolving field of investigation, and future experiments should help settle the interpretation of the density of states modulations both at $H = 0$ and $H \neq 0$. It should be noted that because translational symmetry is broken by the vortices or the pinning centers, there is no fundamental symmetry distinction between the quasiparticle and the pinned-fluctuating-order contributions; nevertheless, their separate spectral and spatial features should allow us to distinguish them.

V. A PHASE DIAGRAM WITH COLLINEAR SPINS, BOND ORDER, AND SUPERCONDUCTIVITY

We have already discussed two experimental possibilities for the coupling g in Fig 1, which we used to tune the ground state of the doped Mott insulator between various distinct phases: the doping concentration, δ , and the strength of a magnetic field, H , applied perpendicular to the layers. A simple phase diagram in the small H region as a function of these parameters was presented in Fig 12, and its implications were compared with a number of experiments in Sections IV.A and IV.D. However, even though it is experimentally accessible, the field H induces a large scale spatial modulation associated with the vortex lattice, and is consequently an inconvenient choice for microscopic theoretical calculations. Here we follow the strategy of introducing a third theoretical axis, which we denote schematically by \tilde{g} , to obtain a global view of the phase diagram. As we argue below, information on the phases present as a function of \tilde{g} sheds considerable light on the physics as a function of H .

The crucial role of order parameters characterizing Mott insulators in our discussion suggests that we should work with a coupling, \tilde{g} , which allows exploration of different ground states of Mott insulators already at $\delta = 0$. The range of this coupling should obviously include regimes where the Mott insulator has the magnetically ordered ground state of Fig 3a, found in La_2CuO_4 . Now imagine adding further neighbor couplings in (5) which frustrate this magnetic order, and eventually lead

¹⁰ Also, Ichioka *et al.* (2001) studied the vortex lattice in a state with pre-existing long-range collinear spin order

to a phase transition to a paramagnetic state.¹¹ As discussed in Section III.C.1, it was argued (Read and Sachdev, 1989b, 1990; Sachdev and Park, 2002) that any paramagnetic state so obtained should have bond order, most likely in the patterns in Figs 6a and b.

It would clearly be useful to have numerical studies which tune a coupling \tilde{g} acting in the manner described above. *Large scale* computer studies of this type have only appeared recently. The first results on a quantum antiferromagnet which has a spin of $S = 1/2$ per unit cell, whose Hamiltonian maintains full square lattice symmetry, and in which it is possible to tune a coupling to destroy the collinear magnetic order, were obtained recently by Sandvik *et al.* (2002). Their model extended (5) with a plaquette ring-exchange term, and had only a U(1) spin rotation symmetry. Theoretical extensions to this case have also been discussed (Lannert *et al.*, 2001; Park and Sachdev, 2002). Along with the collinear magnetic state in the small ring-exchange region (small \tilde{g}), Sandvik *et al.* (2002) found the bond-ordered paramagnetic state of Fig 6a in the large ring-exchange region (large \tilde{g}).

A second large scale computer study of the destruction of collinear magnetic order on a model with $S = 1/2$ per unit cell was performed recently by Harada *et al.* (2003). They generalized the spin symmetry group from SU(2) to SU(N); in our language, they used the value of N as an effective \tilde{g} . They also found the bond order of Fig 6a in the paramagnetic region.

These theoretical studies give us confidence in the theoretical phase diagram as a function of \tilde{g} and δ sketched in Fig 13 (Sachdev and Read, 1991; Vojta, 2002; Vojta and Sachdev, 1999; Vojta *et al.*, 2000a). Phase diagrams with related physical ingredients, but with significant differences, appear in the work of Kivelson *et al.* (1998) and Zaanen (1999).

Important input in sketching Fig 13 was provided by theoretical studies of the effects of doping the bond-ordered paramagnetic Mott insulator at large \tilde{g} . In this region without magnetic order, it was argued that a systematic and controlled study of the doped system was provided by a generalization of the SU(2) spin symmetry¹² to Sp(2 N), followed by an expansion in $1/N$. This approach directly gives (Sachdev and Read, 1991) a stable bond-ordered state at $\delta = 0$, a stable d -wave superconductor at large δ , and a region in which these two orders co-exist at small values of δ ; all of these phases are nicely in accord with the overall philosophy of the present

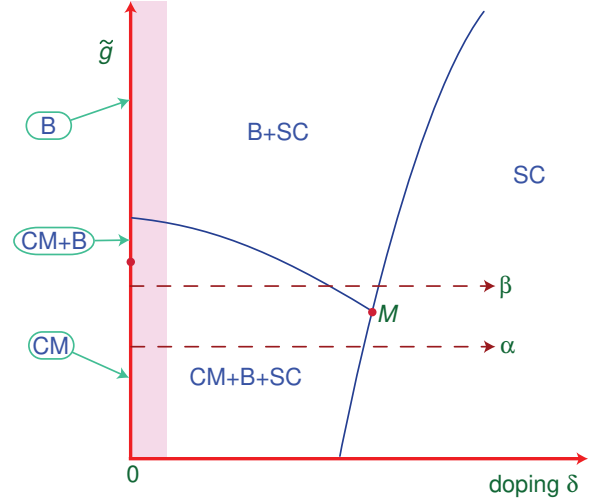


FIG. 13 Zero temperature, zero magnetic field phase diagram as a function of the doping δ , and a coupling constant \tilde{g} . Here \tilde{g} is, in principle, any coupling which can destroy the collinear magnetic order at (π, π) in the undoped insulator, while the Hamiltonian maintains full square lattice symmetry with spin $S = 1/2$ per unit cell. The states are labeled by the orders which exhibit long-range correlations: collinear magnetic (CM), bond (B) and d -wave-like superconductivity (SC). At $\delta = 0$, the CM order is as in Fig 3a, the B order is as in Fig 6a or b, and we have assumed a co-existing CM+B region, following Sachdev and Park (2002) and Sushkov *et al.* (2001). The ground state will remain an insulator for a small range of $\delta > 0$ (induced by the long-range Coulomb interactions), and this is represented by the shaded region. The CM order for $\delta > 0$ could be as in Fig 3b or c, and the B order as in Figs 6a, b, c, or d, but a variety of other periods are also possible (Vojta, 2002; Vojta and Sachdev, 1999). The dashed line α indicates the path followed in Fig 12 at $H = 0$, but the physical situation could also lie along line β . A number of other complex phases are possible in the vicinity of the multicritical point M ; these are not shown but are discussed in Zhang *et al.* (2002), Zaanen *et al.* (2001), and Zaanen and Nussinov (2002) and also, briefly, in Section VI.

article. This analysis of a model with purely short-range interactions also found a phase separation instability at small values of δ (Sachdev and Read, 1991), whose importance had been emphasized by others (Bang *et al.*, 1991; Emery *et al.*, 1990) on different grounds. With long-range Coulomb interactions no macroscopic phase separation is possible, and we have to deal with the physics of frustrated phase separation (Emery *et al.*, 1990). The interplay between bond order and d -wave superconductivity has been studied in some detail in this region (Vojta, 2002; Vojta and Sachdev, 1999; Vojta *et al.*, 2000a): more complex bond ordered structures with large periods can appear, usually co-existing with superconductivity (as sketched in Fig 13). Predictions were made for the evolution of the ordering wavevector with δ , and the period 4 structures in Figs 6c and d were found to be especially stable over a wide regime of doping and parameter space.

¹¹ We assume that there is no intermediate state with non-collinear magnetic order, as this is not supported by observations so far.

¹² The group SU(2) is identical to the symplectic group Sp(2), but the group SU(2 N) is distinct from Sp(2 N) for $N > 1$. Consequently, distinct $1/N$ expansions are generated by models with SU(2 N) or Sp(2 N) symmetry. The Sp(2 N) choice better captures the physics discussed in this article, for reasons explained in Sachdev and Read (1991).

The phase diagram of Fig 13 also includes a region at small \tilde{g} , with collinear magnetic order, which is not directly covered by the above computations. “Stripe physics” (Machida, 1989; Poilblanc and Rice, 1989; Schulz, 1989; Zaanen and Gunnarsson, 1989)—the accumulation of holes on sites which are anti-phase domain walls between Néel ordered regions—is associated with this region. However, these stripe analyses treat the magnetic order in a static, classical manner, and this misses the physics of valence bond formation that has been emphasized in our discussion here. A related feature is that their domain walls are fully populated with holes and are insulating. Upon including quantum fluctuations accounting for valence bonds, it appears likely to us that the stripes will have partial filling (Kivelson and Emery, 1996; Nayak and Wilczek, 1997), acquire bond order, and co-exist with superconductivity, as has been assumed in our phase diagram in Fig 13. Indeed, as we have emphasized throughout, it may well be that the modulation in the site charge density—which is proportional to $Q_a(\vec{r})$ with $\vec{r}_a = 0$ in (10)—is quite small, and most of the modulation is for $\vec{r}_a \neq 0$.

The reader should now be able to use the perspective of the phase diagram in Fig 13 to illuminate our discussion of experiments in Section IV. The phase diagram in Fig 12, used to analyze neutron scattering experiments in Section IV.A and STM experiments in Section IV.D, has its horizontal axis along the line labeled α in Fig 13; the phases that appear in Fig 12 as a function of increasing H should be related to those in Fig 13 as a function of increasing \tilde{g} , although the detailed location of the phase boundaries is surely different.¹³ The absence of topological order in the experiments discussed in Section IV.B, is seen in Fig 13 to be related to the absence of states with non-collinear spin correlations or topological order. The formation of $S = 1/2$ moments near non-magnetic impurities is understood by the proximity of confining, bond-ordered phases in Fig 13. The possible signals of bond order in a superconductor at $H = 0$ in the STM observations of Howald *et al.* (Howald *et al.*, 2003, 2002), may be related to the B+SC phase along the line β in Fig 13; similarly, the observations of Hoffman *et al.* (Hoffman *et al.*, 2002a) at $H \neq 0$ can be interpreted by the proximity of the B+SC phase at $H = 0$.

VI. OUTLOOK

The main contention of this article is that cuprate superconductors are best understood in the context of a phase diagram containing states characterized by the pairing order of BCS theory, along with orders associ-

ated with Mott insulators; the evidence so far supports the class of Mott insulators with collinear spins and bond order. The interplay of these orders permits a rich variety of distinct phases, and the quantum critical points between them offer fertile ground for developing a controlled theory for intermediate regimes characterized by multiple competing orders. This approach has been used to analyze and predict the results of a number of recent neutron scattering, fluxoid detection, NMR, and STM experiments, as we have discussed in Sections IV.A, IV.B, IV.C, and IV.D. Further experimental tests have also been proposed, and there are bright prospects for a more detailed, and ultimately quantitative, confrontation between theory and experiment.

All of the experimental comparisons here have been restricted to very low temperatures. The theory of crossovers near quantum critical points also implies interesting anomalous dynamic properties at finite temperature (Sachdev, 1999; Sachdev and Ye, 1992), but these have not been discussed. However, we did note in Section IV.A that the transition involving loss of magnetic order in a background of superconductivity was a natural candidate for explaining the singular temperature and frequency dependence observed in the neutron scattering at $\delta \approx 0.14$. (Aeppli *et al.*, 1997)

There have also been several recent experimental proposals for a quantum critical point in the cuprates at $\delta \approx 0.19$, linked to anomalous quasiparticle damping (Valla *et al.*, 1999), thermodynamic (Tallon and Loram, 2001), or magnetic (Panagopoulos *et al.*, 2003, 2002) properties. The study of Panagopoulos and collaborators presents evidence for a spin glass state below the critical doping, and this is expected in the presence of disorder at dopings lower than that of the point M in Fig 13.

Among theoretical proposals, a candidate for a quantum critical point (Sachdev and Morinari, 2002; Zaanen *et al.*, 2001; Zhang *et al.*, 2002) at large dopings is a novel topological transition which can occur even in systems with collinear spin correlations. While the topological order present in systems with non-collinear spin correlation leads to fractionalization of the electron (as discussed in Section IV.B), the collinear spin case exhibits a very different and much less disruptive transition in which the electron retains its integrity, but the spin and charge collective modes fractionalize into independent entities. Note that this fractionalization transition was not explicitly shown in Fig 13, and is associated with an additional intermediate state which may appear near the point M. Other theoretical proposals for quantum critical points are linked to the bond/charge order (Kivelson *et al.*, 1998; Seibold *et al.*, 1998) in Fig 13, to order associated with circulating current loops (Chakravarty *et al.*, 2001; Varma, 1997) which has not been discussed in this paper, and to a time-reversal symmetry breaking transition (Khveshchenko and Paaske, 2001; Laughlin, 1998; Sangiovanni *et al.*, 2001; Vojta *et al.*, 2000b) between $d_{x^2-y^2}$ and $d_{x^2-y^2} + id_{xy}$ superconductors. This last

¹³ More precisely, generalizing the arguments leading to (12) and (13), we can state that the system is characterized by an effective g which increases linearly with $H \ln(1/H)$, and an effective δ which decreases linearly with $H \ln(1/H)$

proposal offers a possible explanation of the quasiparticle damping measurements (Valla *et al.*, 1999). Note that this transition does not involve any order associated with the Mott insulator. Indeed, the $d_{x^2-y^2} + id_{xy}$ order can be understood entirely within the framework of BCS theory, and experimental support for $d_{x^2-y^2} + id_{xy}$ superconductivity in recent tunnelling experiments (Dagan and Deutscher, 2001) appears in the overdoped regime, well away from the Mott insulator.

Acknowledgments

I have benefited from discussions and collaborations with many physicists: here I would like to especially thank Gabriel Aeppli, Henri Alloul, Robert Birgeneau, Seamus Davis, Eugene Demler, Matthew Fisher, Aharon Kapitulnik, Steve Kivelson, Christos Panagopoulos, Kwon Park, Anatoli Polkovnikov, T. Senthil, Matthias Vojta, Jan Zaanen, and Ying Zhang for valuable interactions in recent years. This article is based on the F. A. Matsen Endowed Regents Lecture on the Theories of Matter at the University of Texas at Austin, October 2002. This research was supported by US NSF Grant DMR 0098226.

References

Aeppli, G., T. E. Mason, S. M. Hayden, H. A. Mook, and J. Kulda, 1997, *Science* **278**, 1432.

Affleck, I., and J. B. Marston, 1988, *Phys. Rev. B* **37**, 3774.

Alloul, H., P. Mendels, H. Casalta, J.-F. Marucco, and J. Arabski, 1991, *Phys. Rev. Lett.* **67**, 3140.

Altman, E., and A. Auerbach, 2002, *Phys. Rev. B* **65**, 104508.

Andersen, B. M., P. Hedegard, and H. Bruus, 2002, eprint cond-mat/0209061.

Anderson, P. W., 1959, *Phys. Rev.* **115**, 2.

Anderson, P. W., 1987, *Science* **235**, 1196.

Anderson, P. W., 2002, eprint cond-mat/0201431.

Arovas, D. P., A. J. Berlinsky, C. Kallin, and S.-C. Zhang, 1997, *Phys. Rev. Lett.* **79**, 2871.

Balents, L., M. P. A. Fisher, and C. Nayak, 1999, *Phys. Rev. B* **60**, 1654.

Bang, Y., G. Kotliar, C. Castellani, M. Grilli, and R. Raimondi, 1991, *Phys. Rev. B* **43**, 13724.

Bardeen, J., L. N. Cooper, and J. R. Schrieffer, 1957, *Phys. Rev.* **108**, 1175.

Baskaran, G., and P. W. Anderson, 1988, *Phys. Rev. B* **37**, 580.

Bednorz, J. G., and K. A. Müller, 1986, *Z. Phys. B* **64**, 188.

Bobroff, J., H. Alloul, W. A. MacFarlane, P. Mendels, N. Blanchard, G. Collin, and J.-F. Marucco, 2001, *Phys. Rev. Lett.* **86**, 4116.

Bonesteel, N. E., 1989, *Phys. Rev. B* **40**, 8954.

Bonn, D. A., J. C. Wynn, B. W. Gardner, Y.-J. Lin, R. Liang, W. N. Hardy, J. R. Kirtley, and K. A. Moler, 2001, *Nature* **414**, 887.

Byers, J. M., M. E. Flatté, and D. J. Scalapino, 1993, *Phys. Rev. Lett.* **71**, 3363.

Chakravarty, S., B. I. Halperin, and D. R. Nelson, 1989, *Phys. Rev. B* **39**, 2344.

Chakravarty, S., R. B. Laughlin, D. Morr, and C. Nayak, 2001, *Phys. Rev. B* **63**, 94503.

Chen, H.-D., J.-P. Hu, S. Capponi, E. Arrigoni, and S.-C. Zhang, 2002, *Phys. Rev. Lett.* **89**, 137004.

Chen, Y., and C. S. Ting, 2002, *Phys. Rev. B* **65**, 180513.

Chubukov, A. V., S. Sachdev, and J. Ye, 1994a, *Phys. Rev. B* **49**, 11919.

Chubukov, A. V., T. Senthil, and S. Sachdev, 1994b, *Phys. Rev. Lett.* **72**, 2089.

Chubukov, A. V., T. Senthil, and S. Sachdev, 1994c, *Nucl. Phys. B* **426**, 601.

Clay, R. T., S. Mazumdar, and D. K. Campbell, 2002, *J. Phys. Soc. Japan* **71**, 1816.

Coldea, R., D. A. Tennant, A. M. Tsvelik, and Z. Tyliczynski, 2001, *Phys. Rev. Lett.* **86**, 1335.

Cooper, L. N., 1956, *Phys. Rev.* **104**, 1189.

Dagan, Y., and G. Deutscher, 2001, *Phys. Rev. Lett.* **87**, 177004.

Demler, E., C. Nayak, H.-Y. Kee, Y.-B. Kim, and T. Senthil, 2002, *Phys. Rev. B* **65**, 155103.

Demler, E., S. Sachdev, and Y. Zhang, 2001, *Phys. Rev. Lett.* **87**, 067202.

Dombre, T., and G. Kotliar, 1989, *Phys. Rev. B* **39**, 855.

Emery, V. J., S. A. Kivelson, and H. Q. Lin, 1990, *Phys. Rev. Lett.* **64**, 475.

Fazekas, P., and P. W. Anderson, 1974, *Philos. Mag.* **30**, 23.

Fendley, P., R. Moessner, and S. L. Sondhi, 2002, *Phys. Rev. B* **66**, 214513.

Finkelstein, A. M., V. E. Kataev, E. F. Kukovitskii, and G. B. Teitelbaum, 1990, *Physica C* **168**, 370.

Fradkin, E., and S. A. Kivelson, 1990, *Mod. Phys. Lett. B* **4**, 225.

Franz, M., D. E. Sheehy, and Z. Tesanovic, 2002, *Phys. Rev. Lett.* **88**, 257005.

Ghosal, A., C. Kallin, and A. J. Berlinsky, 2002, *Phys. Rev. B* **66**, 214502.

Gonzalez-Buxton, C., and K. Ingersent, 1998, *Phys. Rev. B* **57**, 14254.

Harada, K., N. Kawashima, and M. Troyer, 2003, *Phys. Rev. Lett.* **90**, 117203.

Hoffman, J. E., E. W. Hudson, K. M. Lang, V. Madhavan, H. Eisaki, S. Uchida, and J. C. Davis, 2002a, *Science* **295**, 466.

Hoffman, J. E., K. McElroy, D.-H. Lee, K. M. Lang, H. Eisaki, S. Uchida, and J. C. Davis, 2002b, *Science* **297**, 1148.

Howald, C., H. Eisaki, N. Kaneko, M. Greven, and A. Kapitulnik, 2003, *Phys. Rev. B* **67**, 014533.

Howald, C., H. Eisaki, N. Kaneko, and A. Kapitulnik, 2002, eprint cond-mat/0201546.

Hsu, T., J. B. Marston, and I. Affleck, 1991, *Phys. Rev. B* **43**, 2866.

Ichioka, M., and K. Machida, 2002, *J. Phys. Soc. Japan* **71**, 1836.

Ichioka, M., M. Takigawa, and K. Machida, 2001, *J. Phys. Soc. Japan* **70**, 33.

Julien, M.-H., T. Fehér, M. Horvatic, C. Berthier, O. N. Bakharev, P. Ségransan, G. Collin, and J.-F. Marucco, 2000, *Phys. Rev. Lett.* **84**, 3422.

Katano, S., M. Sato, K. Yamada, T. Suzuki, and T. Fukase, 2000, *Phys. Rev. B* **62**, 14677.

Khaykovich, B., R. J. Birgeneau, F. C. Chou, R. W. Erwin, M. A. Kastner, S.-H. Lee, Y. S. Lee, P. Smeibidl, P. Vorder-

wisch, and S. Wakimoto, 2003, Phys. Rev. B **67**, 054501.

Khaykovich, B., Y. S. Lee, S. Wakimoto, K. J. Thomas, R. Erwin, S.-H. Lee, M. A. Kastner, and R. J. Birgeneau, 2002, Phys. Rev. B **66**, 014528.

Khveshchenko, D., and J. Paaske, 2001, Phys. Rev. Lett. **86**, 4672.

Kishine, J. I., P. A. Lee, and X.-G. Wen, 2001, Phys. Rev. Lett. **86**, 5365.

Kivelson, S. A., 1989, Phys. Rev. B **39**, 259.

Kivelson, S. A., and V. J. Emery, 1996, Synthetic Metals **80**, 151.

Kivelson, S. A., E. Fradkin, and V. J. Emery, 1998, Nature **393**, 550.

Kivelson, S. A., E. Fradkin, V. Oganesyan, I. P. Bindloss, J. M. Tranquada, A. Kapitulnik, and C. Howald, 2002a, eprint cond-mat/0210683.

Kivelson, S. A., D.-H. Lee, E. Fradkin, and V. Oganesyan, 2002b, Phys. Rev. B **66**, 144516.

Kivelson, S. A., D. S. Rokhsar, and J. P. Sethna, 1987, Phys. Rev. B **35**, 8865.

Lake, B., G. Aeppli, K. N. Clausen, D. F. McMorrow, K. Lefmann, N. E. Hussey, N. Mangkorntong, M. Nohara, H. Takagi, T. E. Mason, and A. Schröder, 2001, Science **291**, 1759.

Lake, B., H. M. Rønnow, N. B. Christensen, G. Aeppli, K. Lefmann, D. F. McMorrow, P. Vorderwisch, P. Smeibidl, N. Mangkorntong, T. Sasagawa, M. Nohara, H. Takagi, *et al.*, 2002, Nature **415**, 299.

Lammert, P. E., D. S. Rokhsar, and J. Toner, 1993, Phys. Rev. Lett. **70**, 1650.

Lammert, P. E., D. S. Rokhsar, and J. Toner, 1995, Phys. Rev. E **52**, 1778.

Lannert, C., M. P. A. Fisher, and T. Senthil, 2001, Phys. Rev. B **63**, 134510.

Laughlin, R. B., 1998, Phys. Rev. Lett. **80**, 5188.

Lee, P. A., and G. Sha, 2003, Solid State Comm. **126**, 71.

Lee, P. A., and X.-G. Wen, 2001, Phys. Rev. B **63**, 224517.

Lee, Y. S., R. J. Birgeneau, M. A. Kastner, Y. Endoh, S. Wakimoto, K. Yamada, R. W. Erwin, S.-H. Lee, and G. Shirane, 1999, Phys. Rev. B **60**, 3643.

Machida, K., 1989, Physica C **158**, 192.

Martin, I., G. Ortiz, A. V. Balatsky, and A. R. Bishop, 2000, Int. J. Mod. Phys. B **14**, 3567.

Mazumdar, S., R. T. Clay, and D. K. Campbell, 2000, Phys. Rev. B **62**, 13400.

Mermin, N. D., 1979, Rev. Mod. Phys. **51**, 591.

Moessner, R., and S. L. Sondhi, 2001, Phys. Rev. Lett. **86**, 1881.

Motrunich, O. I., and T. Senthil, 2002, Phys. Rev. Lett. **89**, 277004.

Nagaosa, N., and P. A. Lee, 1992, Phys. Rev. B **45**, 966.

Nayak, C., and F. Wilczek, 1997, Phys. Rev. Lett. **78**, 2465.

Panagopoulos, C., J. L. Tallon, B. D. Rainford, J. R. Cooper, C. A. Scott, and T. Xiang, 2003, Solid State Comm. **126**, 47.

Panagopoulos, C., J. L. Tallon, B. D. Rainford, T. Xiang, J. R. Cooper, and C. A. Scott, 2002, Phys. Rev. B **66**, 064501.

Park, K., and S. Sachdev, 2001, Phys. Rev. B **64**, 184510.

Park, K., and S. Sachdev, 2002, Phys. Rev. B **65**, 220405.

Parks, R. D. (ed.), 1969, *Superconductivity* (M. Dekker, New York).

Pauling, L., 1949, Proc. Roy. Soc. London, A **196**, 343.

Podolsky, D., E. Demler, K. Damle, and B. I. Halperin, 2002, eprint cond-mat/0204011.

Poilblanc, D., and T. M. Rice, 1989, Phys. Rev. B **39**, 9749.

Polkovnikov, A., S. Sachdev, and M. Vojta, 2002a, in *Proceedings of the 23rd International Conference on Low Temperature Physics*, eprint cond-mat/0208334.

Polkovnikov, A., S. Sachdev, M. Vojta, and E. Demler, 2001, in *Proceedings of Physical Phenomena at High Magnetic Fields-IV*, edited by G. Boebinger, Z. Fisk, L. P. Gor'kov, A. Lacerda, and J. R. Schieffer (World Scientific, Singapore), eprint cond-mat/0110329.

Polkovnikov, A., M. Vojta, and S. Sachdev, 2002b, Phys. Rev. B **65**, 220509.

Rantner, W., and X.-G. Wen, 2001, Phys. Rev. Lett. **86**, 3871.

Read, N., and B. Chakraborty, 1989, Phys. Rev. B **40**, 7133.

Read, N., and S. Sachdev, 1989a, Nucl. Phys. B **316**, 609.

Read, N., and S. Sachdev, 1989b, Phys. Rev. Lett. **62**, 1694.

Read, N., and S. Sachdev, 1990, Phys. Rev. B **42**, 4568.

Read, N., and S. Sachdev, 1991, Phys. Rev. Lett. **66**, 1773.

Rokhsar, D. S., and S. A. Kivelson, 1988, Phys. Rev. Lett. **61**, 2376.

Sachdev, S., 1992, Phys. Rev. B **45**, 389.

Sachdev, S., 1999, *Quantum Phase Transitions* (Cambridge University Press, Cambridge).

Sachdev, S., 2000, Science **288**, 475.

Sachdev, S., 2003, Annals of Phys. **303**, 226.

Sachdev, S., and T. Morinari, 2002, Phys. Rev. B **66**, 235117.

Sachdev, S., and K. Park, 2002, Annals of Phys. **298**, 58.

Sachdev, S., and N. Read, 1991, Int. J. Mod. Phys. B **5**, 219.

Sachdev, S., and N. Read, 1996, Phys. Rev. Lett. **77**, 4800.

Sachdev, S., and M. Vojta, 2000, in *Proceedings of the XIII International Congress on Mathematical Physics*, edited by A. Fokas, A. Grigoryan, T. Kibble, and B. Zegarlinski (International Press, Boston), eprint cond-mat/0009202.

Sachdev, S., and J. Ye, 1992, Phys. Rev. Lett. **69**, 2411.

Sandvik, A. W., S. Daul, R. R. P. Singh, and D. J. Scalapino, 2002, Phys. Rev. Lett. **89**, 247201.

Sangiovanni, G., M. Capone, S. Caprara, C. Castellani, C. D. Castro, and M. Grilli, 2001, eprint cond-mat/0111107.

Scalapino, D. J., 1995, Phys. Rep. **250**, 329.

Schollwöck, U., S. Chakravarty, J. O. Fjærstad, J. B. Marston, and M. Troyer, 2002, eprint cond-mat/0209444.

Schulz, H., 1989, J. de Physique **50**, 2833.

Seibold, G., C. Castellani, C. D. Castro, and M. Grilli, 1998, Phys. Rev. B **58**, 13506.

Senthil, T., and M. P. A. Fisher, 2000, Phys. Rev. B **62**, 7850.

Senthil, T., and M. P. A. Fisher, 2001a, Phys. Rev. Lett. **86**, 292.

Senthil, T., and M. P. A. Fisher, 2001b, Phys. Rev. B **63**, 134521.

Shraiman, B. I., and E. D. Siggia, 1988, Phys. Rev. Lett. **61**, 467.

Shraiman, B. I., and E. D. Siggia, 1989, Phys. Rev. Lett. **62**, 1564.

Sidis, Y., C. Ulrich, P. Bourges, C. Bernhard, C. Niedermayer, L. P. Regnault, N. H. Andersen, and B. Keimer, 2001, Phys. Rev. Lett. **86**, 4100.

Sisson, D. L., S. G. Doettinger, A. Kapitulnik, R. Liang, D. A. Bonn, and W. N. Hardy, 2000, Phys. Rev. B **61**, 3604.

Sonier, J. E., J. H. Brewer, R. F. Kiefl, R. I. Miller, G. D. Morris, C. E. Stronach, J. S. Gardner, S. R. Dunsiger, D. A. Bonn, W. N. Hardy, R. Liang, and R. H. Heffner, 2001, Science **292**, 1692.

Sushkov, O. P., J. Oitmaa, and Z. Weihong, 2001, Phys. Rev. B **63**, 104420.

Tallon, J. L., and J. W. Loram, 2001, Physica C **349**, 53.

Thouless, D. J., 1987, Phys. Rev. B **36**, 7187.

Thouless, D. J., 1998, *Topological Quantum Numbers in Non-relativistic Physics* (World Scientific, Singapore).

Tranquada, J. M., J. D. Axe, N. Ichikawa, A. R. Moodenbaugh, Y. Nakamura, and S. Uchida, 1997, Phys. Rev. Lett. **78**, 338.

Tranquada, J. M., J. D. Axe, N. Ichikawa, Y. Nakamura, S. Uchida, and B. Nachumi, 1996, Phys. Rev. B **54**, 7489.

Tranquada, J. M., B. J. Sternlieb, J. D. Axe, Y. Nakamura, and S. Uchida, 1995, Nature **375**, 561.

Tsuei, C. C., and J. R. Kirtley, 2000, Rev. Mod. Phys. **72**, 969.

Valla, T., A. V. Fedorov, P. D. Johnson, B. O. Wells, S. L. Hulbert, Q. Li, G. D. Gu, and N. Koshizuka, 1999, Science **285**, 2110.

Varma, C. M., 1997, Phys. Rev. B **55**, 14554.

Vojta, M., 2002, Phys. Rev. B **66**, 104505.

Vojta, M., and R. Bulla, 2002, Phys. Rev. B **65**, 014511.

Vojta, M., and S. Sachdev, 1999, Phys. Rev. Lett. **83**, 3916.

Vojta, M., Y. Zhang, and S. Sachdev, 2000a, Phys. Rev. B **62**, 6721.

Vojta, M., Y. Zhang, and S. Sachdev, 2000b, Phys. Rev. Lett. **85**, 4940.

Wakimoto, S., R. J. Birgeneau, Y. S. Lee, and G. Shirane, 2001, Phys. Rev. B **63**, 172501.

Wakimoto, S., G. Shirane, Y. Endoh, K. Hirota, S. Ueki, K. Yamada, R. J. Birgeneau, M. A. Kastner, Y. S. Lee, P. M. Gehring, and S. H. Lee, 1999, Phys. Rev. B **60**, 769.

Wang, Q.-H., and D.-H. Lee, 2003, Phys. Rev. B **67**, 020511.

Wen, X.-G., 1991, Phys. Rev. B **44**, 2664.

Wen, X.-G., 2002a, Phys. Rev. B **65**, 165113.

Wen, X.-G., 2002b, Phys. Rev. Lett. **88**, 011602.

Wen, X.-G., and P. A. Lee, 1996, Phys. Rev. Lett. **76**, 503.

White, S. R., and D. J. Scalapino, 1998a, Phys. Rev. Lett. **80**, 1272.

White, S. R., and D. J. Scalapino, 1998b, Phys. Rev. Lett. **81**, 3227.

White, S. R., and D. J. Scalapino, 1999, Phys. Rev. B **60**, 753.

Withoff, D., and E. Fradkin, 1990, Phys. Rev. Lett. **64**, 1835.

Wynn, J. C., D. A. Bonn, B. W. Gardner, Y.-J. Lin, R. Liang, W. N. Hardy, J. R. Kirtley, and K. A. Moler, 2001, Phys. Rev. Lett. **87**, 197002.

Zaanen, J., 1999, Physica C **317**, 217.

Zaanen, J., and O. Gunnarsson, 1989, Phys. Rev. B **40**, 7391.

Zaanen, J., and Z. Nussinov, 2002, eprint cond-mat/0209441.

Zaanen, J., O. Y. Osman, H. V. Kruis, Z. Nussinov, and J. Tworzydlo, 2001, Phil. Mag. B **81**, 1485.

Zachar, O., S. A. Kivelson, and V. J. Emery, 1998, Phys. Rev. B **57**, 1422.

Zhang, D., 2002, Phys. Rev. B **66**, 214515.

Zhang, S.-C., 1997, Science **275**, 1089.

Zhang, Y., E. Demler, and S. Sachdev, 2002, Phys. Rev. B **66**, 094501.

Zhu, J.-X., I. Martin, and A. R. Bishop, 2002, Phys. Rev. Lett. **89**, 067003.